Lawrence Berkeley National Laboratory
Recent Work

Title

EFFECT OF INDIUM AND SILICON DOPING OF THE DEFORMATION BEHAVIOR OF GaAs SINGLE CRYSTALS

Permalink

https://escholarship.org/uc/item/2w8294d3

Author

Tabache, M.G.

Publication Date

1986

eScholarship.org Powered by the California Digital Library
University of California

LBL-20947 c.1

UC-25
LBL-20947

EFFECT OF INDIUM AND SILICON DOPING ON THE DEFORMATION BEHAVIOR OF GaAs SINGLE CRYSTALS

M.G. Tabache
(M.S. Thesis)

January 1986

RECEIVED
LAWRENCE
BERKELEY LABORATORY
1986
LIBRARY AND
DOCUMENTS SECTION

For Reference
Not to be taken from this room

cam

Center for Advanced Materials

Lawrence Berkeley Laboratory
University of California
Berkeley, California 94720

Prepared for the U.S. Department of Energy
under Contract DE-AC03-76SF00098

LBL-20947 c.1

DISCLAIMER

This document was prepared as an account of work sponsored by the United States Government. While this document is believed to contain correct information, neither the United States Government nor any agency thereof, nor the Regents of the University of California, nor any of their employees, makes any warranty, express or implied, or assumes any legal responsibility for the accuracy, completeness, or usefulness of any information, apparatus, product, or process disclosed, or represents that its use would not infringe privately owned rights. Reference herein to any specific commercial product, process, or service by its trade name, trademark, manufacturer, or otherwise, does not necessarily constitute or imply its endorsement, recommendation, or favoring by the United States Government or any agency thereof, or the Regents of the University of California. The views and opinions of authors expressed herein do not necessarily state or reflect those of the United States Government or any agency thereof or the Regents of the University of California.

LBL-20947

EFFECT OF INDIUM AND SILICON DOPING ON THE DEFORMATION BEHAVIOR OF GaAs SINGLE CRYSTALS

Micheline Genevieve Tabache

Department of Materials Science and Mineral Engineering and
Center for Advanced Materials
Lawrence Berkeley Laboratory, University of California
Berkeley, California 94720

January 1986

This work was supported by the Director, Office of Energy Research, Office of Basic Energy Sciences, Materials Science Division of the U. S. Department of Energy under Contract DE-AC03-76SF00098.

ABSTRACT

Doping melt-grown GaAs with high concentrations of indium or silicon has been reported to drastically reduce the dislocation densities, from 10^3 - 10^6 cm^{-2} to less than 10^2 cm^{-2}. To study the effect of doping on the deformation behavior of GaAs single crystals, dynamical compression tests at constant strain rate are performed for temperatures ranging from 350°C to 1100°C. For T > 800°C, samples are encapsulated in B_2O_3. The crystals were grown by the Liquid Encapsulated Czochralski (LEC) technique under identical experimental conditions. Compared to the undoped material, indium-doped GaAs is harder at high temperatures, whereas GaAs:Si is softer. The results show that In and Si behave differently with respect to the deformation tests.

ACKNOWLEDGMENTS

I am very grateful to Professor Eugene Haller for his support and judicious supervision of this work, and for his encouragement.

I am deeply indebted to Dr. Edith Bourret for her sound advice and suggestions, and for her constant availability. Her patience and understanding are gratefully acknowledged.

Dr. Grant Elliot made this work possible by providing the GaAs crystals. I would like to thank him also for his genuine and continuous interest in our work.

The contribution of Professor Eicke Weber whose experience in the field of dislocations and plastic deformation of semiconductor crystals benefited us, is greatly appreciated.

Joe Guitron, Dick Davis and Jeff Beeman have contributed to this work with their technical advice and assistance. I would like to thank Nancy Haegel, John Madok, Joe Kahn and all the members of our group for their various contributions. Special thanks go to Lynne Dory who helped in the editing of the manuscript. Finally, I wish to thank my family for their long-distance unconditional support.

This work was supported by the Director, Office of Energy Research, Office of Basic Energy Sciences, Materials Science Division of the U.S. Department of Energy under Contract DE-AC03-76SF00098.

> "But we ought first to examine ourselves, next the business we wish to undertake, next those for whose sake or with whom we have to act. Above all things, it is necessary to have a proper estimate of oneself, because we usually think that we can do more than we really can."
>
> Seneca, "On tranquility"

TABLE OF CONTENTS

Page

1. Introduction 1

2. Formation of Dislocations During LEC Growth of GaAs Single Crystals. 5

2.1 Generation of dislocations. 6

2.2 Propagation of dislocations 9

2.3 Doping. 13

3. Deformation Experiments. 16

3.1 Sample preparation. 16

3.2 Experimental set-up 24

4. Results. 29

4.1 Theory of the yield point 29

4.2 Experimental results. 33

4.2.1 Raw data 33

4.2.2 Statistical evaluation of errors 35

4.2.3 Stress-strain curves 37

4.2.4 $\mathrm{Log}(\tau_{1y}) = f(T^{-1})$. 39

5. Discussion 53

5.1 Dislocations in GaAs. 54

5.2 Effects of doping on dislocation velocity 57

5.3 GaAs:Si 57

5.4 GaAs:In 64

6. Summary and Conclusions. 70

References 73

1. INTRODUCTION

GaAs has become one of the most important materials for optoelectronic and high speed electronic devices. The quality of the substrates remains a subject of much interest since correlations between dislocation density distribution and several key parameters of the IC's fabricated in GaAs are now established, and show the detrimental effect of the dislocations on the IC's performances [1,2].

The two most widely used growth techniques for bulk GaAs, Horizontal Bridgman (HB) and Liquid Encapsulated Czochralski (LEC), yield crystals with dislocation densities ranging from 10^3 to 10^6 cm^{-2} [3]. HB-grown crystals usually contain less dislocations (10^2 - 10^4 cm^{-2}) than the LEC material due to lower thermal stresses during the growth process; but, drawbacks inherent in the process, such as the shape of the boules, contamination from the crucible, etc., make the LEC technique commercially favored at least at the present time.

Formation of dislocations has also been effectively reduced by control of stoichiometry [4] and intentional additions of impurities such as Si or In [5]. In fact, dislocation densities below 2 - 4000 cm^{-2} have not been achieved in large diameter crystals (D > 30 mm) without doping; in particular, In doping is highly effective in this respect [5,6] and does not affect the intrinsic properties of the material [7,8].

It has been stated that the addition of certain dopants "hardens" the GaAs matrix. This work is aimed at investigating the deformation behavior of doped and undoped GaAs single crystals. An attempt is made to relate the mechanical deformation test results with the dislocation generation and multiplication processes during growth.

One question remains unanswered: what is the mechanism of dislocation density reduction by the addition of impurities ? Doping has been known since 1966 to affect the mechanical properties of semiconductor crystals when J. R. Patel and A. R. Chadhuri reported for the first time the strengthening effect of acceptor impurities and the softening effect of donor impurities in Ge [9]. No similar effect of neutral impurities was observed even in the concentration range 10^{19} cm^{-3}. The authors ascribed the behavior of doped Ge to the effect of impurities on the dislocation mobilities.

Similar work has been done on GaAs. The mechanical behavior of GaAs single crystals has been studied in dynamical uniaxial compression [10] or tension [11] at constant strain rate or at constant force rate [12], in static 3-point bending [13], and in 4-point bending [11]. The materials tested were undoped GaAs, Te-, Si- , and Zn-doped GaAs; the concentrations ranged from 1.7×10^{17} to 1.9×10^{18} cm^{-3} for Te, Si, and from 1.1×10^{18} to 5×10^{19} cm^{-3} for Zn. The samples were cut from crystals grown by various techniques (directional crystallization method, gradient-freeze, HB). Finally, the temperatures of the tests were usually below 600°C because of the As loss problem (As being very volatile, will escape from the GaAs for $T > 650$°C).

In view of the very widely diverse conditions, it is quite difficult to compare quantitatively the different results. However, some general tendencies appear:

- Te and Si doping "harden" GaAs single crystals (i.e., increase the yield stress) as compared to the undoped material, provided that the concentrations are high enough ($> 10^{18}$ cm^{-3}).

- Zn doping on the other hand, tends to "soften" GaAs as compared to the undoped material, but this effect is small, if detected at all.

These effects of doping on the mechanical behavior of GaAs single crystals have been generally attributed to various mechanisms of blocking the propagation of dislocations: elastic and electrical interactions between dislocations and impurities [10,13] or impurity-defect complexes [12]. This is because plastic deformation of semiconductor single crystals can be explained on the basis of the dynamical behavior of dislocations (see Ch. 4). Doping is thought to affect the velocity of individual dislocations, as has been confirmed by numerous experimental studies. The mechanism of this effect is exposed in Chapter 5. Dislocation velocities in undoped GaAs, and Te-, Si-, and Zn-doped GaAs have been measured by double-etch techniques [14-17] or x-ray transmission topography [18]. Three different types of dislocations have been identified in compound semiconductors (see Ch. 5): the screw dislocation, the 60° α dislocation and the 60° β dislocation. All the authors agree that their velocities, as well as the dependence of the velocities on temperature, stress and doping, are different. Therefore, it is difficult to make a correlation between plastic deformation and motion of individual dislocations because it is not known what type(s) of dislocations actually carry(s) out the macroscopic deformation. Steinhardt and Haasen [17] were the first to report a simultaneous investigation of individual dislocation motion and macroscopic plastic flow. They came to the conclusion that at least two types of dislocations participate in the plastic deformation, with different contributions. One important point in their

study is that Zn doping, which "softens" GaAs single crystals also increases the velocity of the two slowest types of dislocations by a factor of 100 to 250, which agrees with the results of Choi, et al. [16]. The mechanisms suggested above to explain the effects of doping on the deformation behavior of GaAs single crystals cannot account for an increase in the velocities because the interactions between dislocations and impurity-related defects generally reduce the velocities of dislocations.

Mechanisms other than blocking of the dislocations have also been mentioned in the literature:

- Seki, et al. [19] ascribe the effect of doping on the velocities of dislocations in GaAs to the strength of the bonds formed between the substitutional impurity atoms and the host atoms surrounding them. Strong bonds will prevent the propagation of dislocations by pinning them at the impurity position. The single-bond energies for impurities in GaAs can be obtained by using the reported values of single-bond energy and electronegativity. This model predicts that Zn should be a very effective impurity in decreasing the grown-in dislocation density whereas In or Si should not. Experimentally, however, the opposite has been observed [5,6] especially in the case of In.
- Ovenskii, et al. [13,15] suggest that doping may affect the Peierls barrier of GaAs (i.e., the intrinsic resistance of the lattice to the motion of dislocations (see Ch. 2)). For consistency with the experimental observations, the Peierls barriers should vary differently with doping for each of the dislocation types.

- Finally, and this seems to be the consensus today, doping is thought to affect dislocation velocities via an electronic mechanism [17,20,21]. The dislocations in semiconductors are charged and therefore they are associated with energy levels in the bandgap. Doping changes the Fermi energy and thus the charge state of these levels. This mechanism is discussed further in Ch. 5.

Unfortunately, the above-mentioned model cannot be applied to In doping in GaAs since In is isoelectronic with Ga. Indium is known to reduce grown-in dislocation densities in LEC-grown GaAs but, to the best of our knowledge, no deformation study of GaAs:In has been carried out at this time. "What mechanism is involved in the case of In?" is the question which we will try to answer by performing dynamical compression tests on undoped, In- and Si-doped GaAs. All the crystals were grown by the LEC technique under exactly the same conditions (thermal gradient, growth rate, diameter, etc.) to minimize the differences in such parameters as native defects or stoichiometry that might influence the dislocation content and thus the deformation behavior (see Ch. 2). The tests are carried out at constant strain rate--10^{-4} s^{-1}--and for temperatures ranging from 350°C to 1100°C. The As loss problem at high temperatures is overcome by encapsulating the sample in B_2O_3, as explained in Ch. 3.

2. FORMATION OF DISLOCATIONS DURING LEC GROWTH OF GaAs SINGLE CRYSTALS

The problem of the dislocation formation during LEC growth of GaAs single crystals can be separated into two parts:

- Generation of dislocations during growth
- Propagation and multiplication of existing dislocations.

2.1 Generation of dislocations

At least three causes for the generation of dislocations have been identified: (i) thermally induced stresses, (ii) native defects, and (iii) non-stoichiometry.

(i) Thermally induced stresses

During growth, the crystal experiences thermally induced stresses created by the temperature gradient [22]. These stresses are a result of spatially inhomogeneous thermal contractions--since the periphery of the ingot is cooler than the core, it is in tension, putting the core in compression. The term "thermal" stresses is often used for convenience to designate the thermally induced stresses.

If these stresses resolved on the {111}, <110> primary slip system exceed a critical value--the critical resolved shear stress (CRSS), the crystal actually encounters plastic flow and the thermal stresses in excess are relieved by crystallographic glide, which involves propagation and multiplication of dislocations.

The initial formation of dislocations in GaAs pulled from the melt by the LEC technique is partly due to excessive thermal stresses associated with the growth process. Calculations of these thermal stresses, based on temperature distribution during growth [22,23], have been used to generate theoretical dislocation contour maps which are in excellent agreement with experimentally observed dislocation patterns .

Estimates of the CRSS at the melting point can be obtained by extrapolation of data obtained at low temperature: Jordan [22] uses the values of the yield stress of GaAs single crystals, as reported by

Swaminathan and Copley [12], in repeated-yielding experiments of Si-doped GaAs for T = 150°C to 550°C ([Si] = $1.8 \times 10^{18} cm^{-3}$). In a repeated-yielding experiment, the sample is heated to the highest temperature, deformed at a constant strain-rate (in this particular study) to a few tenths of a percent, and then unloaded. The temperature is lowered and the specimen is deformed again. This cycle is repeated at successively lower temperatures until the specimen finally fails. The data of Ref. 12 can be extrapolated to higher temperatures by means of the line of best fit:

$$\log(\sigma_{CRSS}) = 5.83 + \frac{1382}{T}$$

σ_{CRSS} is in dyn/cm^{-2}. For T = 1511 K, $\sigma_{CRSS} \simeq$ 60g/mm^{-2}.

The two models [22,23] lead to similar results and they confirm the important role of thermal stresses in the generation of dislocations during growth. However, as pointed out in Ref. 23, other parameters such as native defects or non-stoichiometry must be taken into account as well.

(ii) Native defects

Duseaux and Jacob [23] find that thermal stresses are not always sufficient to explain the dislocation behavior in the LEC growth of GaAs. In some cases, the experimental results will only agree with the predicted ones if a CRSS of 18 kg/mm^{-2}--roughly 30 times Jordan's estimate--is assumed. They suggest that the CRSS can be considerably affected by the concentration of the native defects, their mobility, and interactions with impurities [24].

In the elemental semiconductors (Si,Ge), the native point defects consist mainly of vacancies and/or interstitials at high temperature. In the case of compound semiconductors, the number of native defect

species is larger since antisite defects can occur--for example, As_{Ga} and Ga_{As} in GaAs. Interaction between native defects and impurities adds to the complexity of their study.

Not only do the native defects affect the CRSS for crystallographic glide, but they can also act as centers for heterogeneous nucleation of dislocations: for instance, vacancy or interstitial nucleation into intrinsic or extrinsic stacking faults respectively which are bounded by dislocation loops. Under the influence of thermal stresses, they can act as Franck-Read sources [24].

It has been suggested that doping acts on dislocation densities by affecting the native defect spectrum, concentration, and mobility, which in turn, could change the values of the CRSS [6,23].

(iii) Non-stoichiometry

The effects of stoichiometry on the dislocation density in GaAs have been known for 20 years [25] and were recently demonstrated in a study on GaAs growth by the HB technique under minimized thermal stress and varying arsenic source temperature [4]. For lightly doped n- and p-type GaAs (free-carrier concentration of about 10^{16} cm^{-3}), a minimum dislocation density of 10^3 cm^{-2} was obtained at an optimum As source temperature of 617 ± 1°C. Deviations from this temperature led to higher dislocation densities (~ 10^5 cm^{-2}) which are comparable to those found in GaAs grown under large thermal stresses [26]. It was also shown that these non-stoichiometry-induced dislocations do not propagate as growth proceeds.

Duseaux and Jacob suggested that stoichiometry affects the CRSS and therefore plays an important role in the formation of dislocations during LEC growth [23]. Lagowski, et al. [26] believe that a corre-

lation exists between Fermi energy and dislocation formation in GaAs. They find that low donor concentrations ($\approx 10^{17}$ cm^{-3}) are effective in eliminating non-stoichiometry-induced dislocations, whereas doping with acceptor impurities has the opposite effect.

The non-stoichiometry dislocations would be created by condensation and interaction of point defects, the relevant defect interaction being controlled by the migration of Ga vacancies. The point defects in GaAs create localized electronic levels, the occupancy (i.e. the charge state) of which is controlled by the Fermi energy. The charge state of the various defects control their concentration, migration, and the probability of interaction.

In summary, it is important to note that stoichiometry is the main factor affecting the dislocation density after the thermal stresses have been minimized.

2.2 Propagation of dislocations

A dislocation moving in a crystal is expected to experience a potential energy of displacement that reflects the lattice periodicity and the discrete nature of the crystal medium [27]. When a dislocation lies at a position of symmetry with respect to the atoms in the slip plane, it is not subjected to any force from an otherwise unstrained lattice. The symmetric configuration corresponds to a minimum potential energy configuration. Between these positions of symmetry, a force opposing the displacement of the dislocation is set up because the atoms in the slip plane on opposite sides of the dislocation, no longer lie in equivalent positions in the periodic field of the plane. This force is due to the misfit energy between the faces of

the slip plane. As the dislocation glides, the potential energy of the crystal changes periodically because of the variation of the misfit energy of the dislocation. The energy of misfit is the sum of all the energies of interaction between the atoms facing one another across the slip plane. Peierls [28] predicted that the displacement potential experienced by a dislocation was periodic, with valleys of minimum potential energy and ridges of maximun potential energy. The energy barrier that the dislocation has to overcome when moving is called the Peierls barrier. It has long been accepted that the height of this barrier is considerable in covalently bonded semiconductors--a low Peierls barrier would hardly allow <110> dislocations to be as straight as they appear in electron microscopy [27,29].

The concept of a Peierls barrier is consistent with the observation that the mobility of dislocations in semiconductors increases rapidly with temperature and therefore is thermally activated [30]. This leads naturally to the concept of kinks and jogs in dislocation lines. At 0°K, a dislocation lying parallel to a Peierls valley is at equilibrium if it lies straight in the bottom of the valley everywhere. However, at finite temperature, the minimum free-energy configuration includes a number of randomly positioned double kinks which increase the entropy of the system. Such kinks, shown in Fig. 1, are formed by thermal fluctuations in the crystals. The concentration of thermal kinks is determined by their free energy of formation.

It should be noted at this point that a kinked dislocation lies in a specific slip plane. Thermal agitation can also cause a dislocation to deviate out of its original slip plane by formation of thermally induced jogs. The formation energy of jogs is much larger than that

of kinks, so the concentration of jogs is less than that of kinks at equivalent temperatures--above a certain temperature. Moreover, the kinks are highly mobile and glide easily by lateral expansion, while jogs can move only by climb which requires diffusion of point defects (vacancies or interstitials).

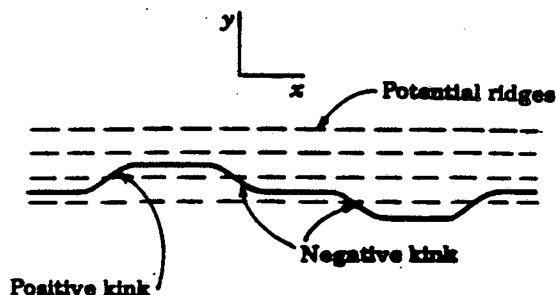

Fig. 1. Double kinks in a dislocation line.

Hirth and Lothe [27] discuss fully the dislocation velocity when it is dominated by double kink nucleation and subsequent expansion. Migration of kinks occurs by shifting of bonds and glide rearrangement of atoms. It is also a thermally activated process, assumed to be controlled by a secondary Peierls potential. According to the model, the velocity of dislocations is proportional to the concentration of kinks, their velocity, and the driving force τ^m, where τ is the resolved shear stress and m a constant ($m \sim 1 \rightarrow 2$). So the velocity can be expressed by:

$$v = A \tau^m \exp(-\frac{E}{kT})$$

where E is the activation energy for the motion of dislocations. E can be stress dependent for low stresses, but this effect can be neglected in a first approximation [16,29]. This expression of v leads to a

good fit for most experimental data on Si, Ge and GaAs [15,16,17,29,31,32].

Dislocations can multiply upon moving via a three-dimensional mechanism [29]. There are essentially two different processes of dislocation multiplication:

- Stationary dislocation sources, for example Frank-Read sources: under an applied stress, a segment of dislocation can bow out by glide between two pinning points. The pinning points can be nodes in a network, sites where the dislocation leaves the glide plane, precipitates etc. For stresses lower than a critical value, a metastable configuration is adopted, in which the line-tension of the dislocation balances the force caused by the stress. When the net local resolved shear stress exceeds the critical value, the expanding loop will anihilate over a portion of its length, creating a complete dislocation loop and the original configuration is restored [27].

- Multiplication of moving dislocations which occurs in proportion to the moving length and the distance travelled via double-cross-slip, kinematic sources mechanisms etc.

In summary, the propagation and multiplication of dislocations during growth are also dependent on the thermal stresses present in the process. Therefore, thermal stresses are an important factor for the grown-in dislocation distribution, although the other factors mentioned earlier cannot be ignored. Measurements of the CRSS as a function of temperature for undoped GaAs and In- and Si-doped GaAs are presented in this study.

2.3 Doping

As mentioned previously, the intentional addition of dopants in the melt provides a very efficient way to reduce the grown-in dislocation density in LEC GaAs. In some cases, large diameter dislocation-free crystals have been obtained. For each dopant, there is a minimum concentration below which no effects are observed. However, for very high concentrations of these dopants, the density is observed to increase again [6]. An optimum range of concentration can be found for each dopant, in which the dopant is most effective in reducing the average density of grown-in dislocations.

Many dopants have been tried and the results are summarized in the following tables:

TABLE 1a.

Group II Elements

Dopant [Ref.]	Concentration (cm^{-3})	Diameter (mm)	EPD* (cm^{-2})
Zn [19]	10^{19}	15 - 25	4000
Zn [6]	10^{20}	20 - 25	8000

*EPD = etch pit density

TABLE 1b.

Group III Elements

Dopant [Ref.]	Concentration (cm^{-3})	Diameter (mm)	EPD (cm^{-2})
B* [5]	10^{19}	15 - 25	10^4–10^5
Al [19]	10^{19}	15 - 25	3000
In [5]	10^{19}	20 - 35	Dislocation-free
In [6]	$2x10^{19}$	20 - 25	100
In [5]	$8x10^{19}$	20 - 25	1000

*Concentration in the melt

TABLE 1c.

Group IV Elements

Dopant [Ref.]	Concentration (cm^{-3})	Diameter (mm)	EPD (cm^{-2})
Si*	$1.5x10^{18}$	50	≃4000
Si*	$3x10^{18}$	50	<100
Sn [6]	$8x10^{18}$	20 - 25	700
Sn [6]	10^{19}	20 - 25	1000

*GaAs:Si used in our studies—see Table 2.

TABLE 1d.

Group V Elements

Dopant [Ref.]	Concentration (cm^{-3})	Diameter (mm)	EPD (cm^{-2})
N [19]	$5x10^{19}$	15 - 25	core is Dislocation-free
P [5]	10^{19}	20 - 25	10^4 - 10^5
P [5]	10^{20}	20 - 25	10^4 - 10^5
Sb [5]	$3x10^{19}$	20 - 25	Dislocation-free

TABLE 1e.

Group VI Elements

Dopant [Ref.]	Concentration (cm^{-3})	Diameter (mm)	EPD (cm^{-2})
Te [19]	$4x10^{18}$	15 - 25	4000
Te [19]	10^{19}	15 - 25	600
Te [6]	$8x10^{18}$-10^{19}	20 - 25	<100
Se [31]	$8.5x10^{18}$	50	few dislocations in the middle
S [31]	$7x10^{18}$	50	few dislocations in the middle

By comparing these data, it appears that the most effective impurities are In, Si, Sn and the group VI elements. However, care must be taken when making comparisons because other parameters such as diameter of the boule, crystallinity and microdefects have to be taken into account. Jacob, _et al_. [33] report that the high concentration of Sb needed to

effectively reduce the average dislocation density makes it difficult to grow a single crystal. They also report that nitrogen doping increases the probability of growing twins. Dislocation-free GaAs obtained by doping with group VI elements have a high concentration of microdefects (loops, stacking faults, etc.) which do not act as sources for macroscopic dislocations [6]. These microdefects have not been observed in Zn-, Al- or N-doped GaAs but these dopants are only weakly efficient in reducing the dislocation density in small crystals. Finally, GaAs:In and GaAs:Si can be grown dislocation-free in large diameter without microdefects. The microdefects introduced in GaAs by heavy doping with certain elements could play a role in the generation and/or the motion of dislocations during growth. This subject needs further investigation.

3. DEFORMATION EXPERIMENTS

3.1 Sample preparation

All the materials tested are LEC grown. Except for the highly dislocated undoped GaAs grown under ill-defined conditions, they are all grown under the same experimental conditions: the growth direction is the <100> direction and the diameter of the boules is 2". The growth rate is 7.5 mm/hr and the thermal stresses were minimized by using a very low temperature gradient (6°C/cm). The characteristics of the materials are given in Table 2.

Etching with $HF:H_2O_2:H_2O$, 1:1:2 for 3 minutes, reveals the dislocations on the (111) Ga face. The dislocations arrangement (aligned on slip lines or arranged in cells) and distribution for each crystal reflect the growth conditions and the effect of doping.

Three areas can be distinguished on the highly dislocated undoped GaAs {111} slice: a) Near the periphery, the dislocations are aligned on three different types of slip lines which correspond to the three <110> directions contained in the plane of the slice (fig. 2a). b) The minimum density is observed between the <110> edges and the center, and there, the density of the dislocations is several thousands per cm^{-2}. The dislocations are arranged in cells of ~ 10 - 1000 μm in diameter enclosing dislocation-free areas (Fig. 2b). The cells are smaller towards the center of the slice. c) In the center the dislocation density is intermediate between a) and b) (fig. 2c).

An etched 111 slice of the second series of undoped GaAs (RD2-301) grown under minimized thermal stresses shows basically the same features, but the dislocation density is much lower, ~ 2 - 3000 cm^{-2} (Fig. 3) and the dislocations at the periphery are aligned along one direction only.

The GaAs:In is practically dislocation-free ($d_{\perp} < 100\ cm^{-2}$) except for an area of about 3 mm at the periphery, where again the dislocations are aligned along the three <110> directions.

The highly doped GaAs:Si (H282) is also dislocation-free, and the few dislocations present at the periphery of the boule are not aligned along slip lines. The second Si-doped GaAs has an average dislocation density of 4 - 6000 cm^{-2} and the dislocations are arranged in cells across the whole surface of the slice. Even at the periphery, the dislocations are not aligned along any direction.

The specimens for our deformation studies are cut into prisms with square bases. The orientation <321> is used as the compression axis

TABLE 2.

Characteristics of the GaAs Crystals

Used for our Deformation studies.

Material*	Intentional Doping Average Concentration (cm^{-3})	Resistivity Average (Ωcm)	EPD** (cm^{-2})
undoped S.R.	-		>10000
undoped RD2-301	-	$7x10^{6}$ (semi-insulating)	2-3000
GaAs:In H276	[In] ≈ $2.9x10^{19}$	$1.8x10^{7}$ (semi-insulating)	<100
GaAs:Si (1) H282	[Si] ≈ $3x10^{18}$	$7.5x10^{-3}$	<100
GaAs:Si (2) RD1-043	[Si] ≈ $1.5x10^{18}$		3-4000

* Hewlett-Packard, OED Division, San Jose, CA

**EPD: etch pit density

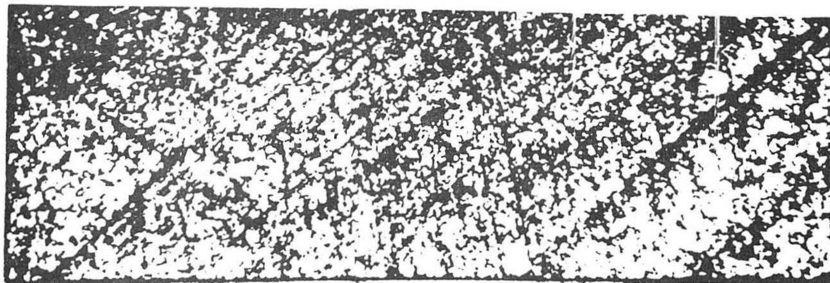

Fig. 2a. Undoped GaAs sample (before deformation) cut near the periphery of the slice (slip lines).

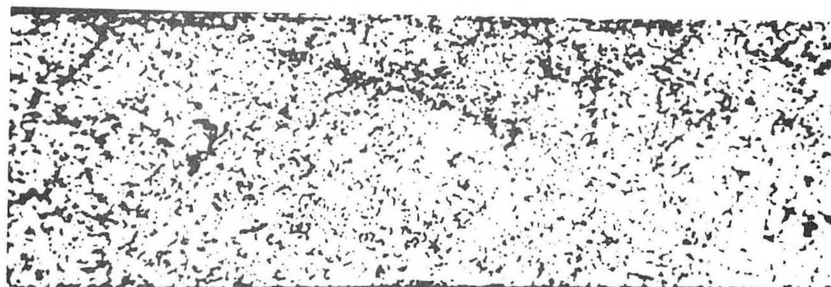

Fig. 2b. Undoped GaAs sample cut in the middle part of the slice (low EPD).

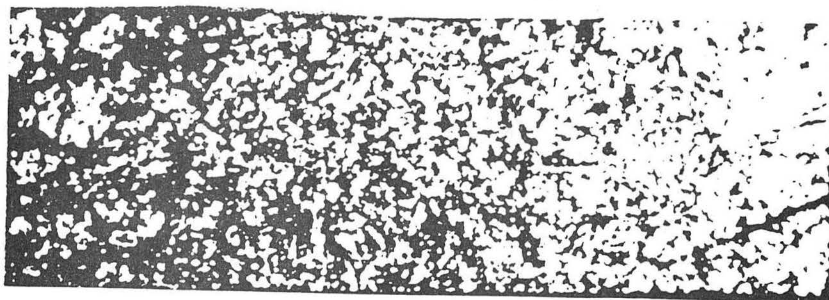

Fig. 2c. Undoped GaAs sample cut in the center of the slice (intermediate EPD).

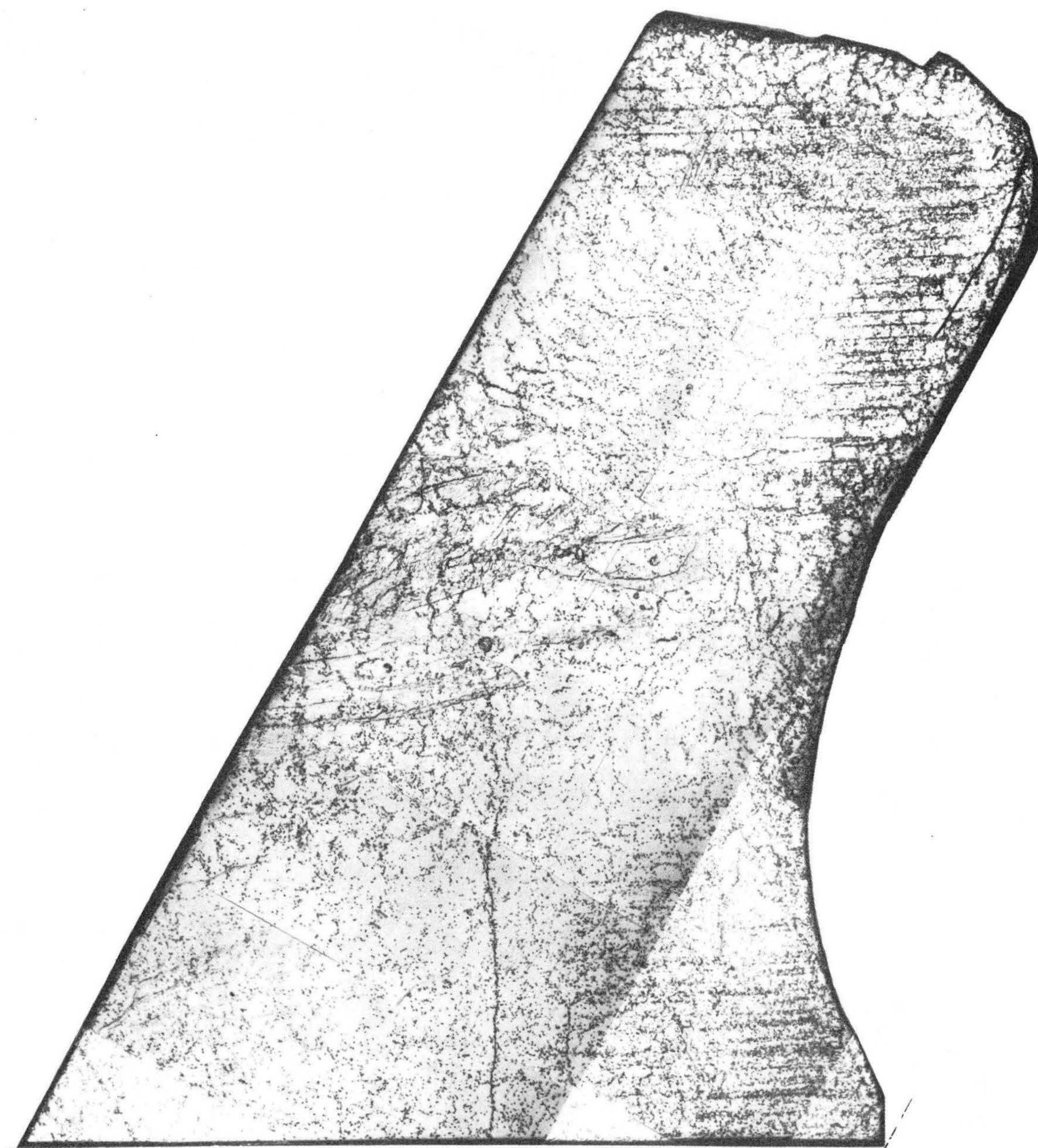

XBB 862-1045

Fig. 3. Dislocation-etched undoped GaAs {111} slice (10x).

because only one slip system operates (Fig. 4); therefore, the deformation of the samples occurs by single slip, which should facilitate the evaluation of the results. The slip system is characterized by a geometrical factor, μ, defined as follows [34]:

$$\mu = \cos\alpha \times \cos\beta$$

where α = angle between compression axis and normal to the slip plane, and β = angle between compression axis and slip direction in the slip plane. For example, in Fig. 4,

$$\mu = \cos([3\bar{2}\bar{1}],[1\bar{1}1]) \times \cos([3\bar{2}\bar{1}],[10\bar{1}])$$

$$\mu = 0.4667$$

μ can take any value between 0 and 0.5--the larger μ is, the easier the slip on this system. So in the case of a $[3\bar{2}\bar{1}]$ compression axis, the first system to operate is $(1\bar{1}1)$, $<10\bar{1}>$. The <321> directions were determined by x-ray Laue reflection. Best results were obtained when a tungsten tube was used and when the surface of the crystal was lapped. We estimate the accuracy of the orientation at ± 2°. The orientation by x-ray reflection is very time-consuming because <321> directions are totally asymmetric directions. Therefore, whenever a direction was known on the {111} slice--the <100> growth direction for instance--the <321> directions were determined by the angles between <100> and <321> (see figure 5). The accuracy of the orientation in this case can be estimated at about ± 4°. This error on the orientation does not affect single slip, because we are still far from the second slip system for which $\mu = 0.35$.

After the $\{\bar{1}11\}$ slice is dislocation-etched and a <321> direction determined, the samples are cut and an enlarged picture (10x) of each individual sample is taken to keep track of its dislocation content.

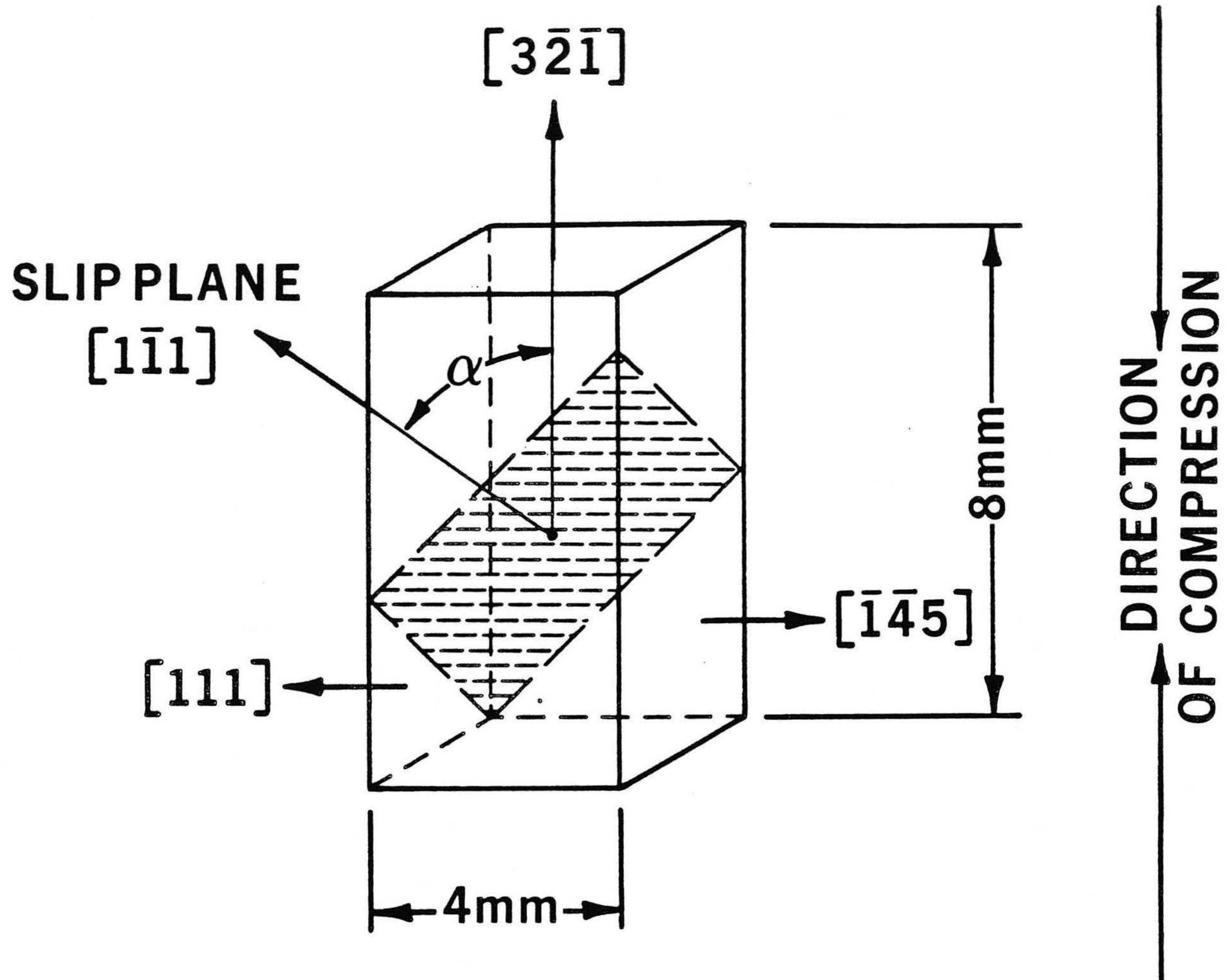

XBL 8511-4646

Fig. 4. GaAs sample for deformation tests
Indexed faces.

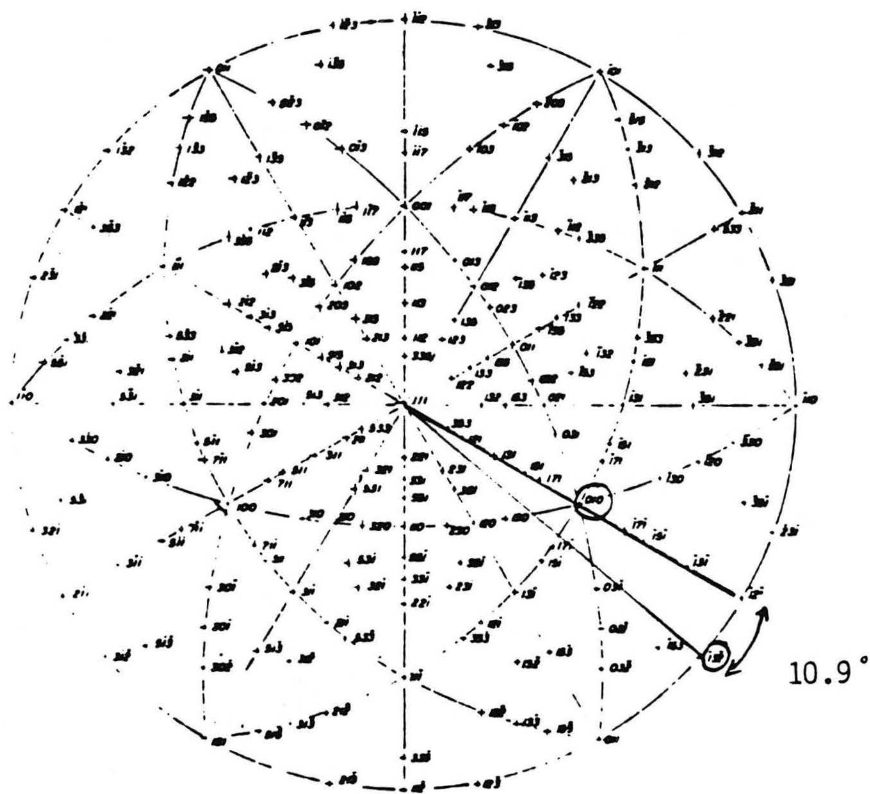

Fig. 5. Detailed {111} stereographic projection.

The samples are then lapped down to size using an aqueous suspension of 3 μm Al_2O_3 particles. The samples are 8 mm long and depending on the availability of the material, the cross-section is 4.5 mm^2 (for undoped GaAs RD2-301 and GaAs:In), or 8.5 mm^2 (for GaAs:Si). The length-to-width ratio l/w is respectively ~ 3.8 and ~ 2.7 but it is reasonable to neglect an effect of this parameter given that it was found to be irrelevant for l/w > 2.0 [12].

Finally, the samples are mechanically-chemically polished in a 2:1:3 solution of colloidal silica dispersion, H_2O_2 and DI H_2O. The parallelism of the end faces, an important factor for the uniformity of the deformation [29], is checked with a micrometer; and the samples whose end faces are not parallel within less 0.1° are discarded. The dimensions of the samples are precisely measured for later reduction of the data (see Ch. 4.2).

3.2 Experimental set-up

Figure 6 is a picture of the set-up. The fixtures are built to fit in a universal testing machine (Instron, model 1122). Figure 7 is a schematic showing the important features:

o The compression load cell (full-range: 0 - 1000 N) is contained in the bottom bellow, and the fixed compression rod rests on top of it. The four openings in the neck of the bellow are used for the monitoring thermocouple (K-type, inconel sheath), the evacuation of the system or the introduction of the argon gas, the pressure and vacuum gauges and finally, the electrical cord of the load cell.

• A three-zone split furnace is used together with a temperature controller, which allows constant heating rates and reproducible temperature cycles.

• The quartz chamber enclosing the compression rods and the sample can be made vacuum tight. For T < 800°C, the sample rests directly on the fixed rod and the monitoring thermocouple is placed at ~ 2 mm away from it (Fig. 8a). For T > 800°C, the sample is placed in an Al_2O_3 crucible and is held strain-free in the upright position by a BN ring (Fig. 8b); B_2O_3 powder with a high hydroxyl content (1200 ppm) to lower its viscosity, covers the ring and the sample. For these tests, another monitoring thermocouple is used. It is attached to the moving compression rod and dips into the liquid B_2O_3 when the compression is actually being carried out.

• The top bellow allows the motion of the cross-head while keeping the system vacuum tight. A blank test proved that the presence of the bellow does not disturb the signal, because the fixtures and the load cell are decoupled.

The actual procedure to carry out a test is as follows: the sample is set in place and the system is closed. The mobile compression rod is brought a few mm above the sample to allow for the substantial thermal expansion of the Al_2O_3 rods. The system is evacuated down to ~ 10^{-3} atm with a mechanical pump. Argon gas is then flushed in, up to a pressure of ~ 2 atm and these last two steps are repeated twice. Then, by opening the corresponding valve, argon flows into the system, exiting at the top of the system through a filter that traps the As, should there be any. The desired temperature is set, and the heating starts. The temperature inside the quartz chamber is recorded, and when a thermal equilibrium is well established, usually in one hour, the compression is carried out. The strain rate is chosen by selecting the cross-head speed; to be closer

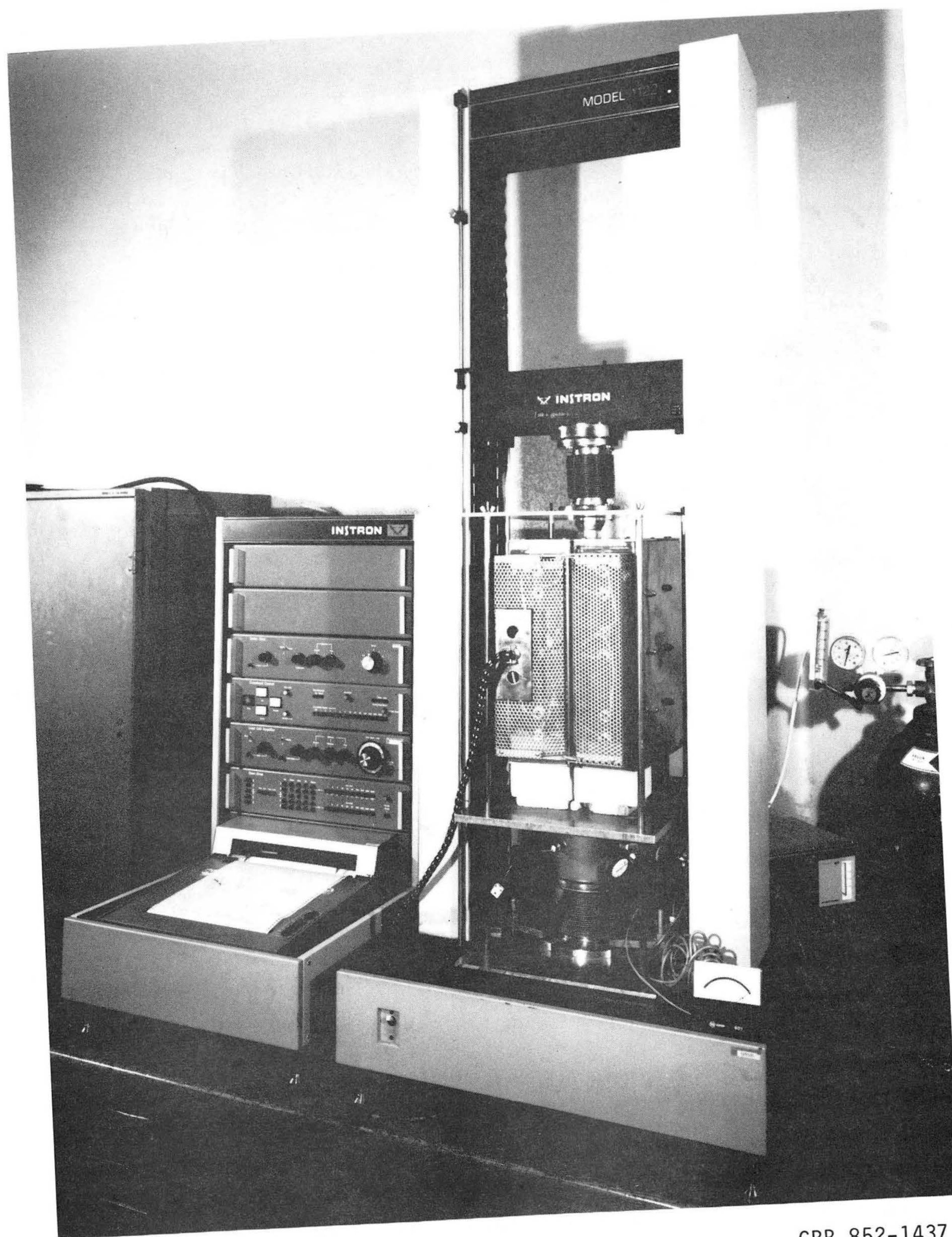

CBB 852-1437

Fig. 6. Picture of the deformation set-up.

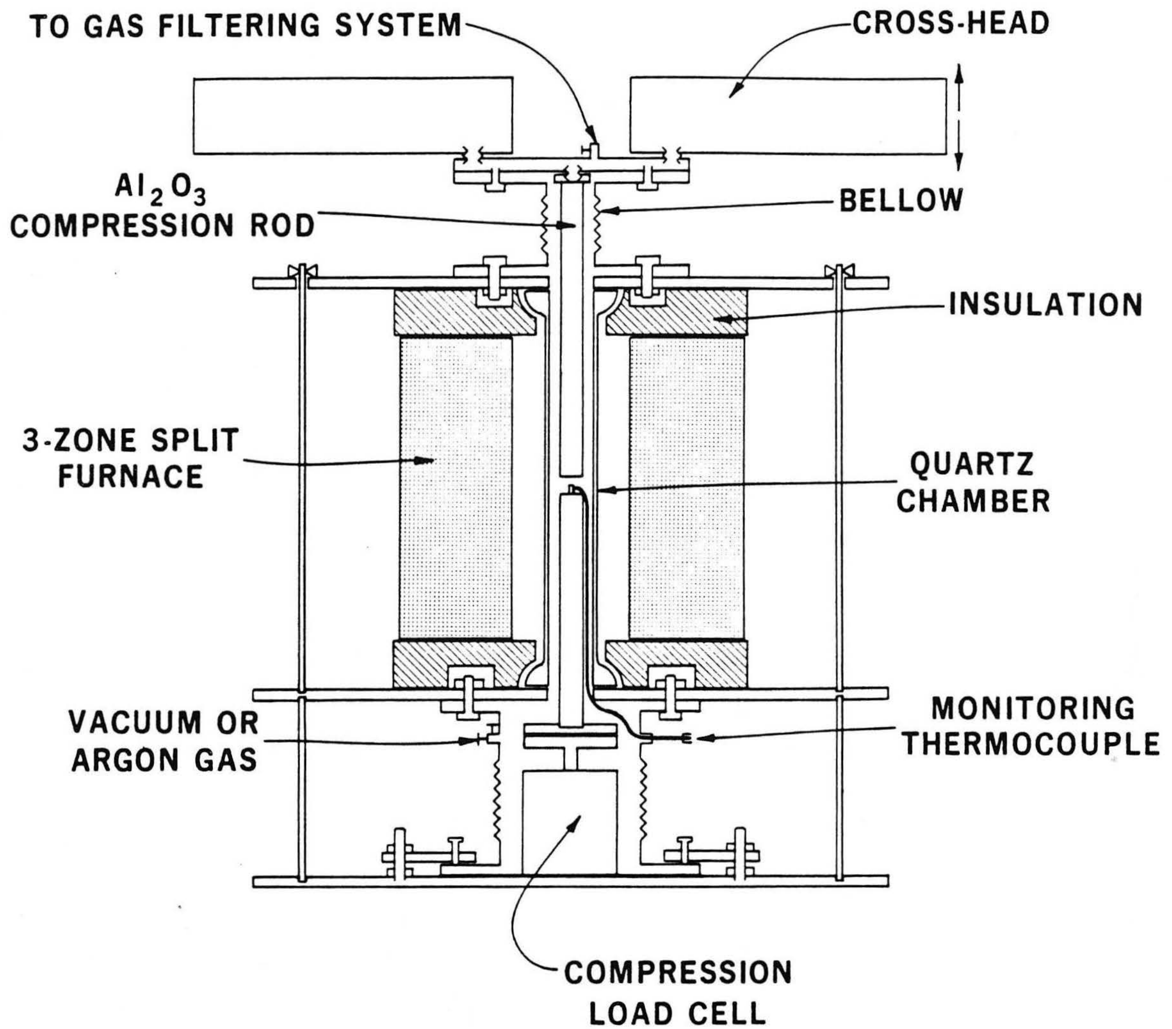

Fig. 7. Schematic of the deformation set-up.

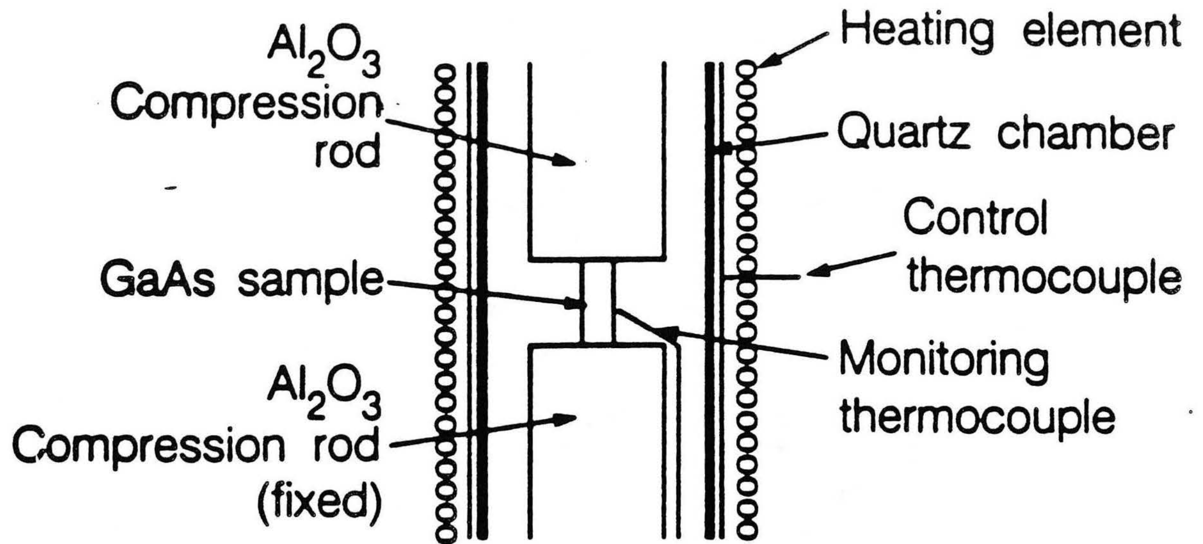

Fig. 8a. Positioming of the sample for the deformation tests.

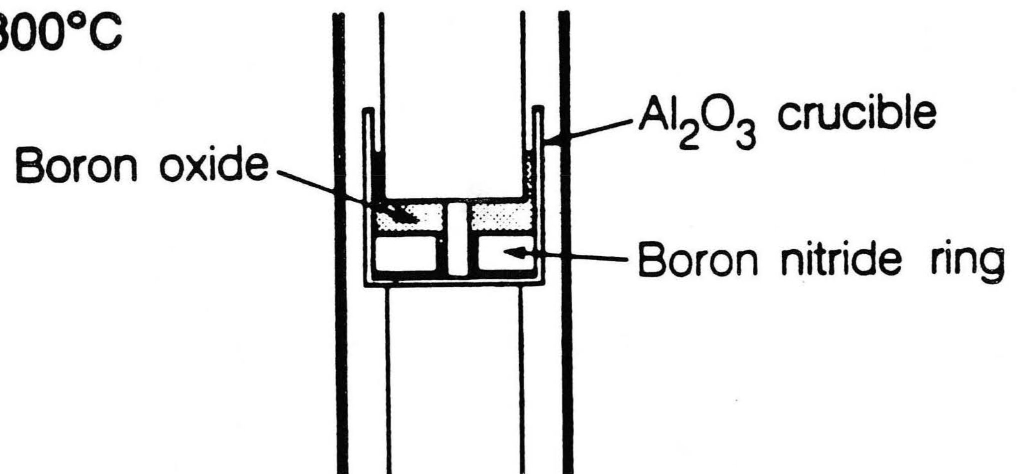

Fig. 8b. Encapsulation for T >800°C

to an equilibrium situation, the slowest speed is used (50 μm/min), and this corresponds to a nominal strain-rate $\dot{\varepsilon}$ of:

$$\dot{\varepsilon} = \frac{\Delta l}{l} \times \frac{1}{\Delta t} = \frac{0.05(mm)}{8\ (mm)} \times \frac{1}{60(s)} \simeq 10^{-4}s^{-1}$$

The weight on the load cell is zeroed out by adjusting the balance right before the compression is started. Once the test is completed, the split furnace is opened and the system allowed to cool to room temperature.

4. RESULTS

4.1 Theory of the yield point

A typical curve is shown in fig.9. After a quasi-linear increase of the stress with increasing strain, the stress drops to a lower level and starts increasing again. The local maximum occuring after the initial linear part is called the upper yield stress and is noted τ_{uy}. The local minimum after the upper yield stress position is the lower yield stress, noted τ_{ly}.

The yield phenomenon common to all semiconductors in dynamical deformation tests at constant strain rate, can be understood on the basis of the dynamical behavior of dislocations during the course of plastic deformation. As early as 1940, Orowan [35] had pointed out that the plastic properties of crystals are governed by the dynamics of dislocation motion and generation, and that the plastic shear strain rate is determined by:

$$\dot{\gamma} = \rho_m \times b \times v$$

where ρ_m is the density of mobile dislocations, b the Burgers vector and v the velocity of these dislocations. The plastic shear strain rate $\dot{\gamma}$ is related to the plastic strain rate $\dot{\varepsilon}$ by: $\dot{\gamma} = \dot{\varepsilon}/\mu$, where μ is the Schmid factor characterizing the slip system. Based on this expression, Haasen developed a theory of the yield point that is widely accepted today [36]. In a crystal with few grown-in dislocations, the specimen produces at the

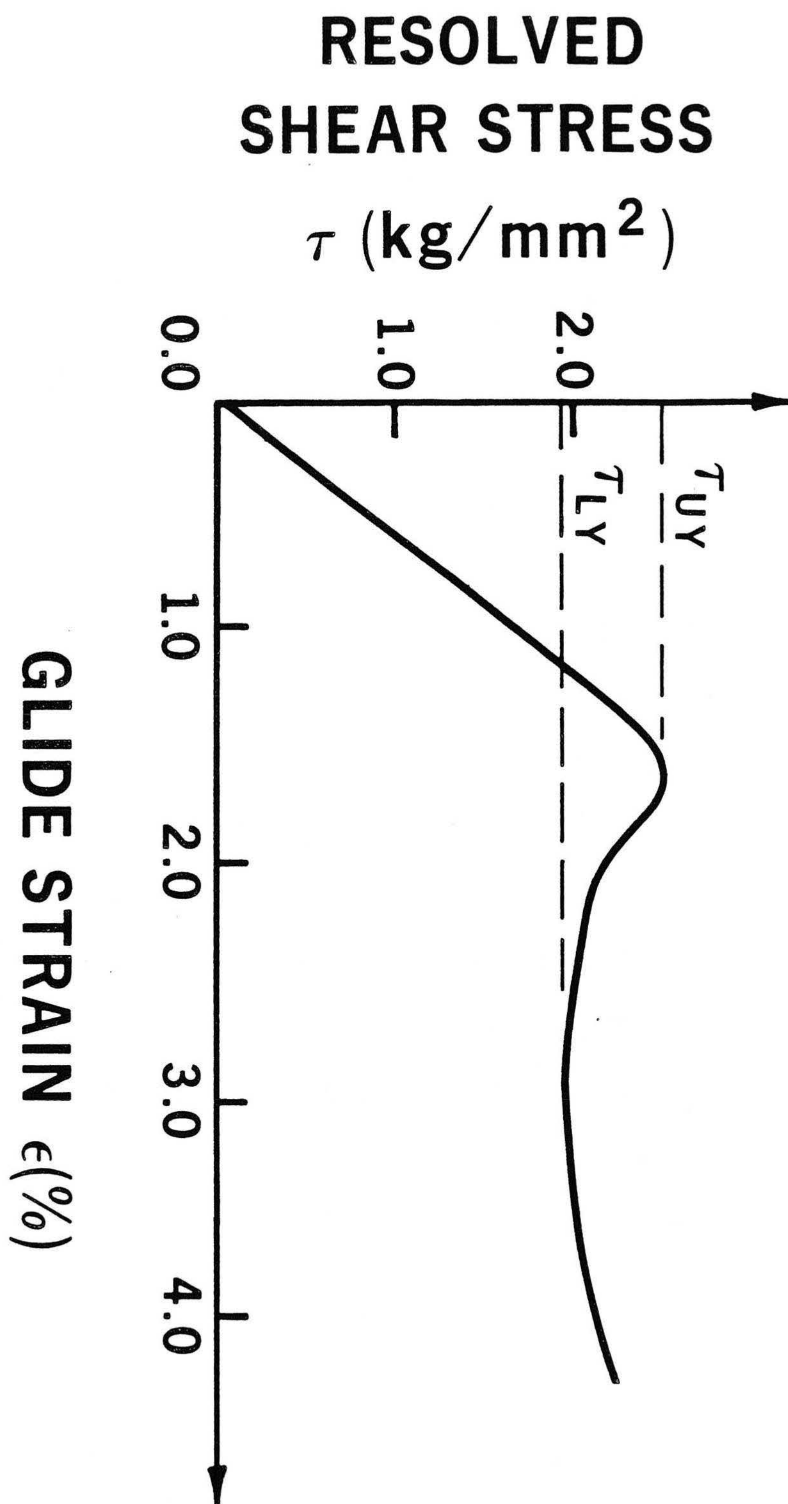

Fig. 9. Typical stress-strain curve in dynamical deformation test of GaAs single crystal.

beginning of the deformation, a high stress that gives the existing dislocations a high velocity (v is proportional to τ^m, m>0, see chapter 2). The few dislocations initially moving then multiply, with the effect that their velocities decrease in accordance with the prescribed strain rate. At about two-thirds of τ_{uy}, the slope $d\tau/d\epsilon$ becomes noticeably smaller, and after the peak at τ_{uy}, the stress falls continuously over a range of ~ 1% and a pronounced minimum is reached at τ_{ly}. The stresses and strains at the upper and lower yield points are determined by the following parameters: machine hardness, strain rate, temperature, orientation and initial dislocation content of the specimen. The machine hardness determines the amount of the cross-head motion that goes into the elastic strain of the doping fixture. After τ_{ly}, dislocation multiplication leads to dislocation interaction and the applied stress must increase again to keep the effective velocity level prescribed by the strain rate.

Three of the five parameters that determine the upper and lower yield points are kept constant for all our experiments: the machine hardness, the orientation of the samples and the strain rate, which is nominally 10^{-4} s^{-1}. That leaves the initial dislocation content and the temperature as relevant parameters.

It is found experimentally that the values of the upper yield stress are not very reliable [11,29,37] because they strongly depend on the initial dislocation content. The preparation of the surfaces and the alignement of the samples become crucial since a flaw on the surface can act as a source for fresh dislocations and deviations from perfect alignement can cause non-uniform slip in the sample. Moreover, the effects of gripping (in tension) or friction (in compression) add to the lack of accuracy observed for τ_{uy} [29].

These are the reasons why the expected decrease of τ_{uy} and of the yield drop ($\tau_{uy}- \tau_{ly}$) with increasing temperature cannot be quantitatively analyzed. They also explain why the strain values ε_{uy} and ε_{ly} are difficult to analyze. These strains and the corresponding shape of the yield drop depend on the whole integrated strain history of the specimen. In general, $\varepsilon_{uy} \simeq 0.05$-$1\%$ and $\Delta\varepsilon \simeq 1\ \%$ and these values should increase with decreasing initial dislocation content.

The lower yield point however, is less affected by all these factors because when this point is reached, the effects of friction and initial dislocation density are reduced.

More significantly than the reasons stated previously, the lower yield point is chosen as the relevant parameter to describe the deformation behavior of the tested materials because τ_{ly} is a good estimate of the CRSS for slip. The formation of macroscopically extended dislocations in semiconductor crystals at high temperature is found to take place at stresses lower than the upper yield point [16,38]. Muller, et al.,reported in a recent paper [39] the study of the deformation behavior and dislocation formation in doped InP. They interrupted the dynamical compression at various stages and subsequently etched the samples; they make the following statement: the onset of the dislocation formation seems to occur at a stress level which lies about 10-20 % below the upper yield point. They also note that the formation of dislocations is increased when the stress exceeds the value of the lower yield stress on the initial slope. This is further support to adopt the value of τ_{ly} as the CRSS, as was suggested by P.Haasen [40].

The expression of the lower yield stress can be derived in the framework of the theory of the yield point [29]. The starting point is

the Orowan formula [35]:

$$\dot{\gamma} = \rho_m \times b \times v$$

where v can be expressed as (see 2.2);

$$v = A \times \tau^m \times \exp(-E/kT)$$

Using the facts that τ goes through a minimum as a function of ρ_m and also as a function of strain, the stress at the lower yield point can be derived. It is:

$$\tau_{ly} = C \times \dot{\varepsilon}^{-(m+2)} \times \exp\left(\frac{E}{(m+2)kT} \right)$$

where E is the activation energy for the dislocation motin and C is a function of the strain rate. Note that E and m in the expression of τ_{ly} represent the same quantities as in v. This theoretical expression is well supported by experiment [9,10,11].

4.2 Results

4.2.1 Raw data

For each material, tests are carried out at various temperatures ranging from 350°C to 1100°C. The Instron machine records the load on the sample as a function of time. In order to compare the behavior of the different samples, the dimensions of the specimens have to be accounted for; therefore, the curves obtained are transformed into resolved shear stress vs percentage glide strain curves.The resolved shear stress (RSS) is the stress acting on a slip plane, in a slip direction. It is given by:

$$RSS = \frac{\text{load}}{\text{initial area}} \times \text{Schmid factor} = \mu \times \frac{P(kg)}{A_0(mm^{-2})}$$

The percentage glide strain at time t is defined by:

$$\varepsilon_t = \frac{\text{elongation at t}}{\text{initial length}} \times 100 = \frac{\Delta l}{l_0} \times 100 = 100\times \frac{\Delta t(min) \times 0.05(mm/min^{-1})}{l_0(mm)}$$

The specimens deformed up to a few percent have an S-shape which indicates that there is no buckling (a barrel shape would result from buckling). Slip lines are apparent on the large faces of the specimens. They are aligned along one direction, which confirms that single slip took place. Figure 10 shows the S-shape and the slip lines on an undoped GaAs sample deformed up to 3.5% at 570°C.

In some cases, the end faces are not "perfectly" parallel and it becomes apparent on the initial portion of the deformation curve, often in the form of a shoulder.

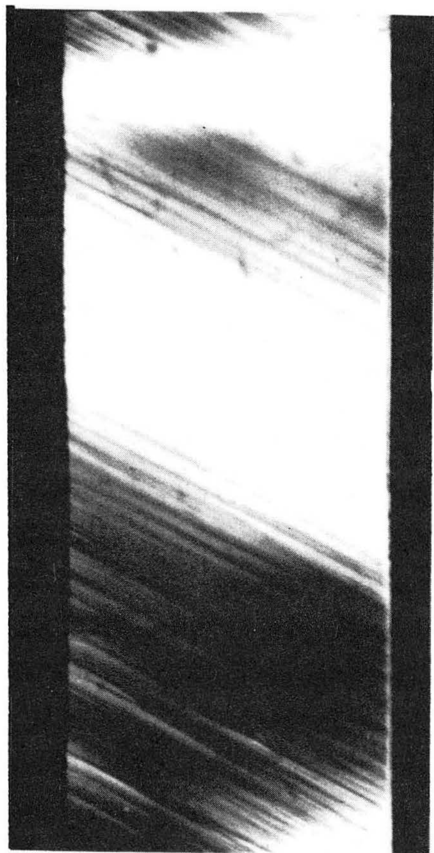

XBB 862-1046

Fig.10. Slip lines after 3.5 % deformation at 570°C.

4.2.2 Statistical evaluation of errors

In order to study the reproducibility of our measurements, and to estimate the error on the numerical values, a series of 15 samples cut out from the same crystal were tested under identical conditions. The samples were cut from a {111} slice of the heavily dislocated undoped GaAs. The dislocation content of each specimen was different depending on the position in the slice. The influence of the dislocation density and structure on the yield stresses and strains is difficult to assess. It was not possible to find a correlation between the dislocation content of the samples and their yield behavior.

Moreover, the temperature for these tests varied between 356°C and 367°C. Because of the exponential dependence of the yield stresses on the temperature, a few degrees difference will markedly affect the yield stresses for this range of temperatures. We estimate that $d\tau_{ly}/dT = 0.02$ kg/(mm^{-2}xK) for this range of temperature; if $\Delta T = 10$ K, then $\Delta \tau_{ly} = 0.2$ kg/mm^{-2}. In some cases, even the variations of the yield stresses and strains with temperature could not be justified, which indicates that the reading of T is accurate within ≈ 2°C (the reading of T depends very much on the exact position of the monitoring thermocouple and of the sample). Greater care in positioning the monitoring thermocouple was taken for subsequent measurements.

In summary, with two parameters that could not be kept precisely constant (initial dislocation content and temperature), the error estimated in this statistical study is the worst case that can happen with our set-up. The error on the upper yield stress is of the order of ±20 %, whereas the error on the lower yield stress is ≈ ±12 %. The results of this study are summarized in table 3.

TABLE 3.

Statistical Study (undoped GaAs, high $d_{\perp}$, T = 356 - 367°C)

	Upper Yield Resolved Shear Stress	Lower Yield Resolved Shear Stress
Minimum Value	2.31 kg/mm^{-2}	1.73 kg/mm^{-2}
Maximum Value	4.61 kg/mm^{-2}	2.92 kg/mm^{-2}
Mean Value	3.41 kg/mm^{2}	2.13 kg/mm^{-2}
Error	± 20%	± .12%
Strains At Yield Point	1.13 -> 1.87%	2.98 -> 4.66%

Strain rate = 10^{-4} s^{-1}

The yield drop ($\tau_{uy} - \tau_{ly}$) varied from 0.24 to 2.06 kg/mm^{-2} and $\Delta\varepsilon = \varepsilon_{uy} - \varepsilon_{ly}$ varied from 1.30 to 3.24% .

In figure 7 of [11], stress-strain curves for tests carried out at 850°C are shown. All samples were cut from the same ingot but their

deformation behavior is quite varied and inconsistent with the initial dislocation density. The authors of [11] also report that in all their tests, the values of τ_{uy} varied "considerably" whereas the values of τ_{ly} are said to vary by less than 10 % . As mentioned previously, reproducibility is a problem always encountered with dynamical tests and is due in part to the initial defect content of the samples. The highly dislocated undoped GaAs was grown under different conditions than the other three materials.

The high defect content of this undoped GaAs made it suitable for the estimates of maximum errors in our measurements; however, because of its different thermal history, it will not be used for comparisons to determine the effect of doping on the deformation behavior. In what follows "undoped" GaAs refers to the undoped GaAs grown under minimized thermal stresses, unless otherwise specified.

4.2.3 Stress-strain curves

Figures 11 to 13 represent typical stress-strain curves for different temperatures. The tests were arbitrarily interrupted after the yield drop, because we are only interested in the first part of the deformation curve. They all show the same general behavior, as described in 4-1. The strain rate is constant and equal to 10^{-4} s^{-1}. There is no curve for GaAs:Si at low temperatures because the samples would break before the upper yield was reached. The theory of the yield point predicts that both yield stresses should decrease with increasing temperature, and this behavior is actually observed in most of the cases; but because of the lack of accuracy of τ_{uy}, the yield drop is sometimes observed to increase with increasing T, where it is expected to decrease (compare for example curves 1 and 2 in figure 12). As for the values of the strains

at the yield points, they generally behave according to the theory, and they decrease with increasing temperatures.

A yield elongation stage is sometimes observed at the lower yield point: the yield drop is followed by a work-hardening-free stage (i.e. the stress stays constant with respect to ε), that Alexander and Haasen [29] attribute to inhomogeneous slip. The theory of the yield point describes stress-strain behavior for homogeneous slip and cannot account for this effect. Inhomogeneous slip is often observed in the first stages of the deformation of diamond-cubic materials where the lattice resistance to dislocation motion is high. Curve 2 in figure 12 shows such a behavior.

Figures 14 and 15 are stress-strain curves for different materials at one temperature. In fig.14, where T = 570°C, the highly doped GaAs:Si has the highest τ_{ly}, followed by GaAs:Si(2), GaAs:In and finally undoped GaAs. This tendency is changed in fig.15, where T = 1080°C; in this case, GaAs:In has the highest τ_{ly} and GaAs:Si(1) the lowest. These effects of doping on the deformation behavior of GaAs appear more clearly in the following figures, that describe the variation of τ_{ly} with temperature. In figs.16-20, the natural logarithm of τ_{ly} is plotted as a function of T^{-1} (K^{-1}) for each material tested. The points on these graphs are aligned and the equations of the lines passing through the points are determined by least-square fit. The results are summarized in table 4.

Note on figures 17 to 20 that the yield stresses determined between 850°C and 950°C tend to be too high. This could be due to the fact that at these temperatures, B_2O_3 is too viscous and disturbs the signal on the load cell.

TABLE 4.

$$\tau_{ly} = A \exp \frac{B}{kT}$$

Material	A (g/mm^{-2})	B (eV)	τ_{ly} at T = Tm (g/mm^{-2})
undoped (high $d_\perp$)	2.96 ± 0.1	0.36 ± 0.02	46.45
undoped (low $d_\perp$)	2.35 ± 0.08	0.37 ± 0.02	40.77
GaAs:Si (1)	0.15 ± 0.006	0.68 ± 0.03	26.95
GaAs:Si (2)	0.79 ± 0.04	0.48 ± 0.03	32.43
GaAs:In	8.05 ± 0.26	0.30 ± 0.01	81.86

4.2.4 Log(τ_{ly}) = f(T^{-1})

(i) undoped GaAs: Figures 16 and 17 represent the variation of Log(τ_{ly}) as a function of T^{-1} for the two undoped GaAs. Although the two materials were very different from their thermal history and their initial defect content point of view, the lines determined by least-square fit are very close. This result confirms the idea that the lower yield stress is not as dependent on the initial dislocation content or on the quality of the surfaces as the upper yield stress. τ_{ly} corresponds to a point where two competing phenomena are equal in intensity: on the one hand, dislocations are multiplying fast and the stress in the sample tends to decrease, but on the other hand, interactions between dislocations are becoming more important and the stress in the sample tends to increase again. When τ_{ly} is reached, many dislocations have been already generated in the deformation process, and the initial condition of the sample

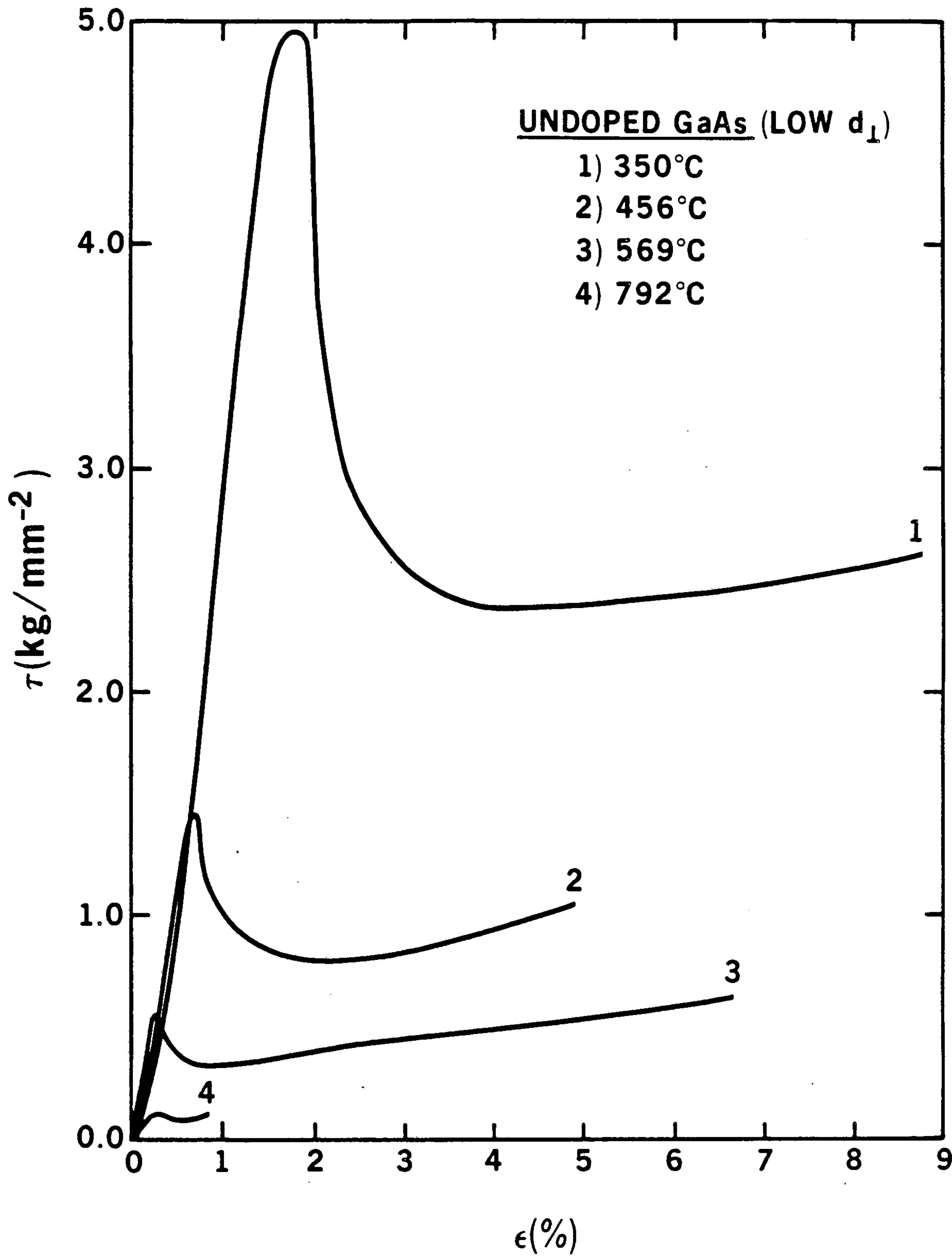

Fig. 11. Typical stress-strain curves for undoped GaAs. Variations with T.

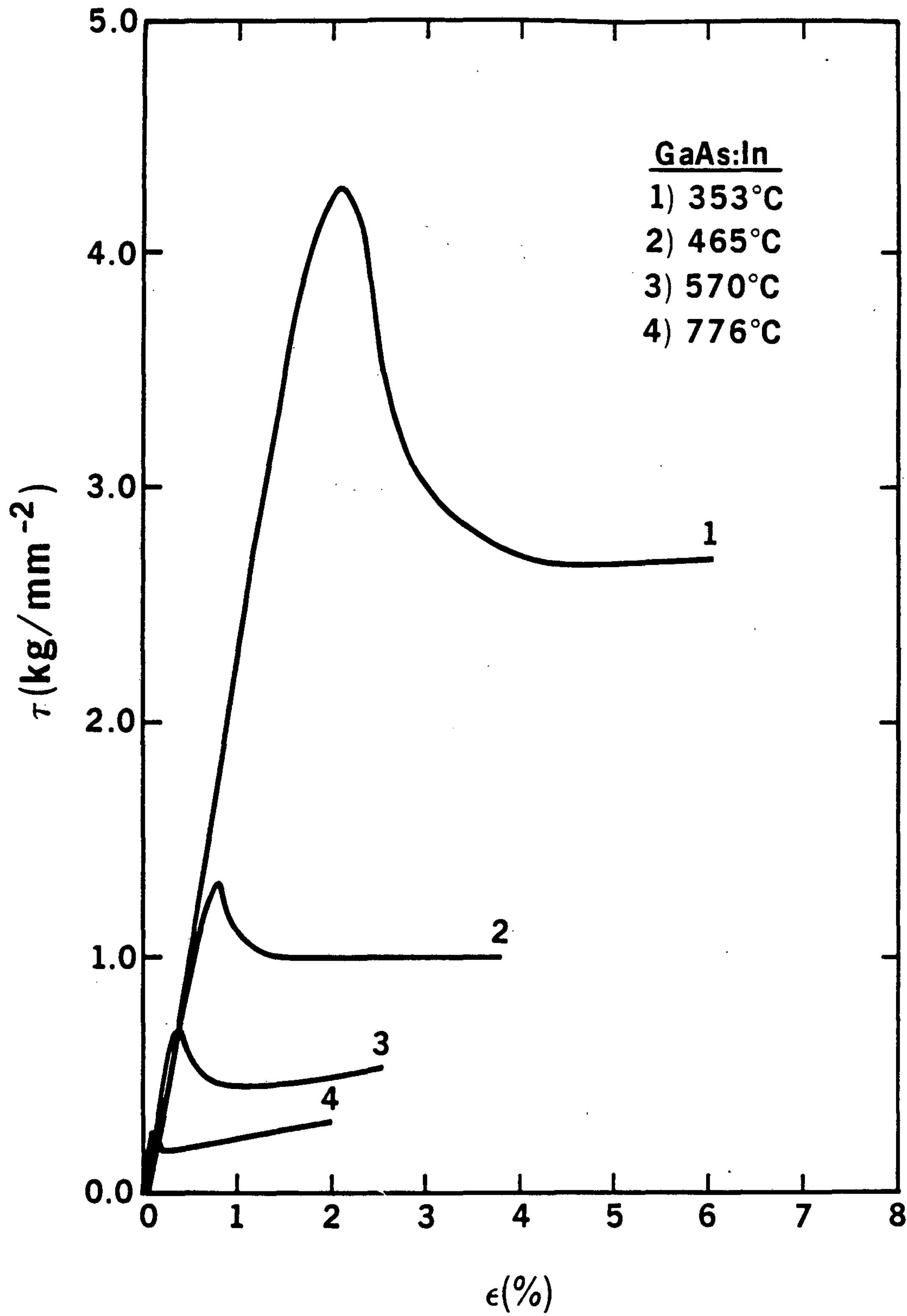

XBL 8511-4642

Fig. 12. Typical stress-strain curves for GaAs:In. Variations with T.

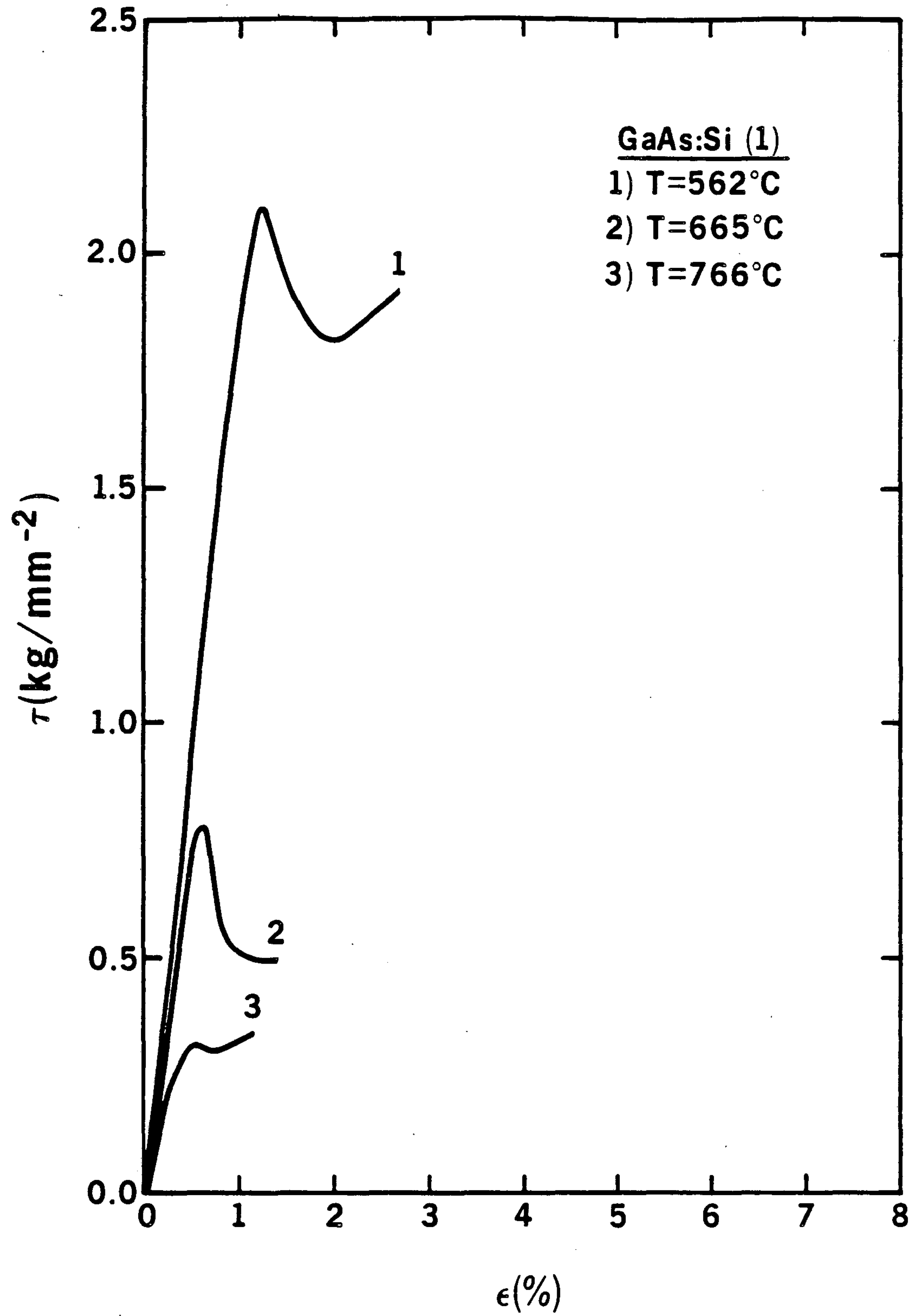

Fig. 13. Typical stress-strain curves for GaAs:Si. Variations with T.

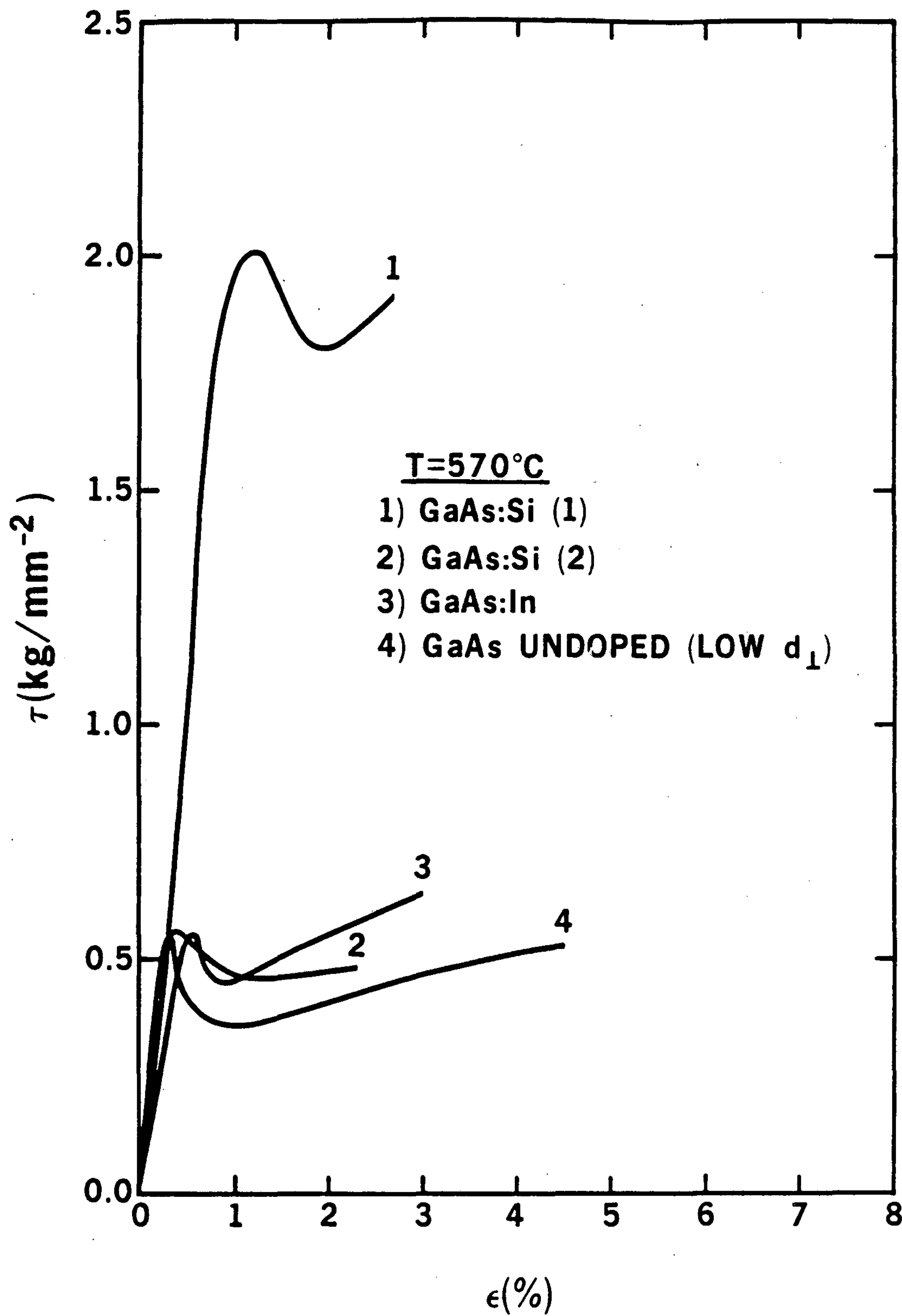

XBL 8511-4632

Fig. 14. Variations of stress-strain curves with dopant. T=570°C.

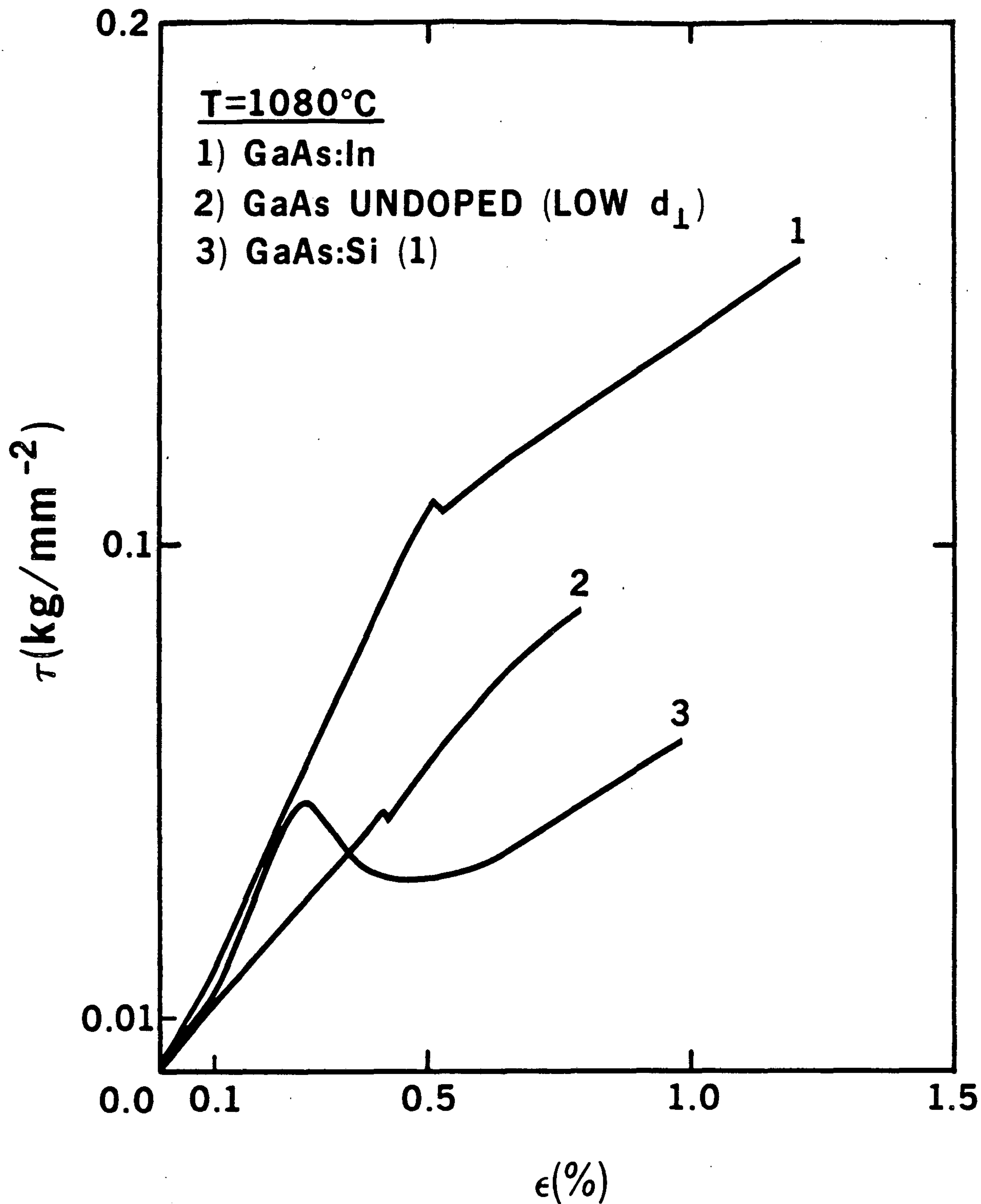

XBL 8511-4631

Fig. 15. Variations of stress-strain curves with dopant. T=1080°C.

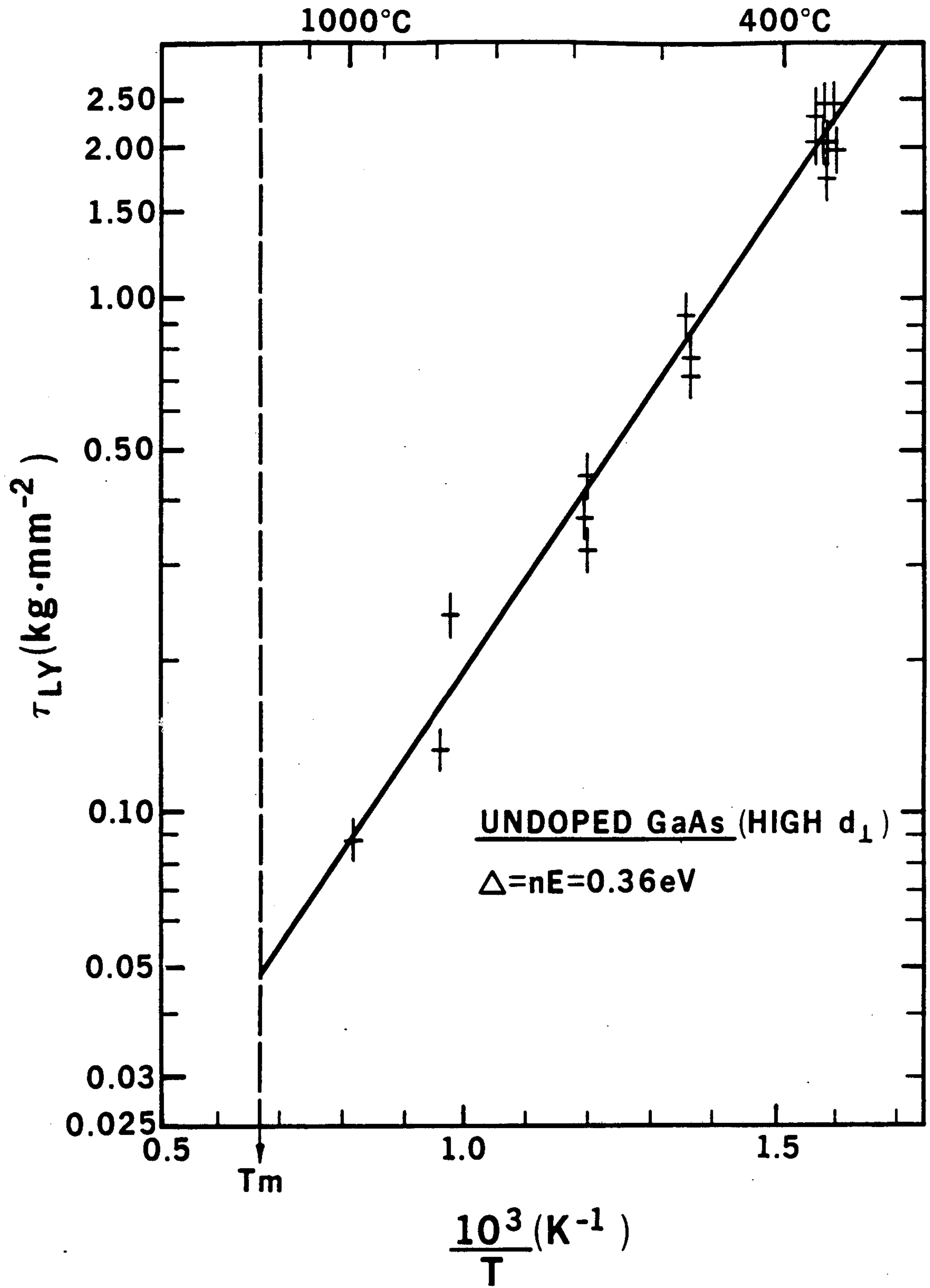

XBL 8511-4637

Fig. 16. Log(τ_{ly}) = f(1/T).
Undoped GaAs (high d).

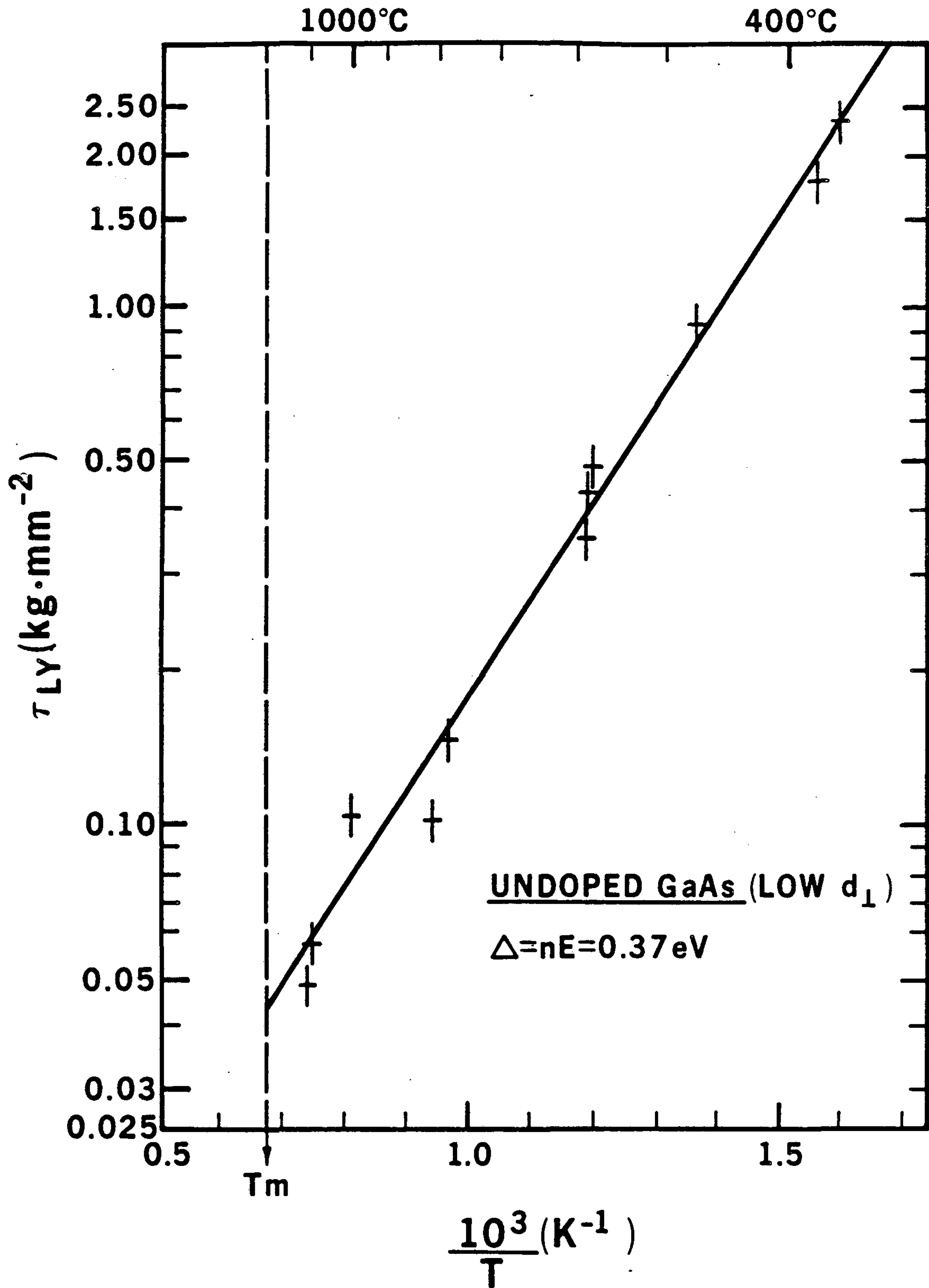

XBL 8511-4635

Fig. 17. Log(τ_{1y}) = f(1/T).
Undoped GaAs (low d).

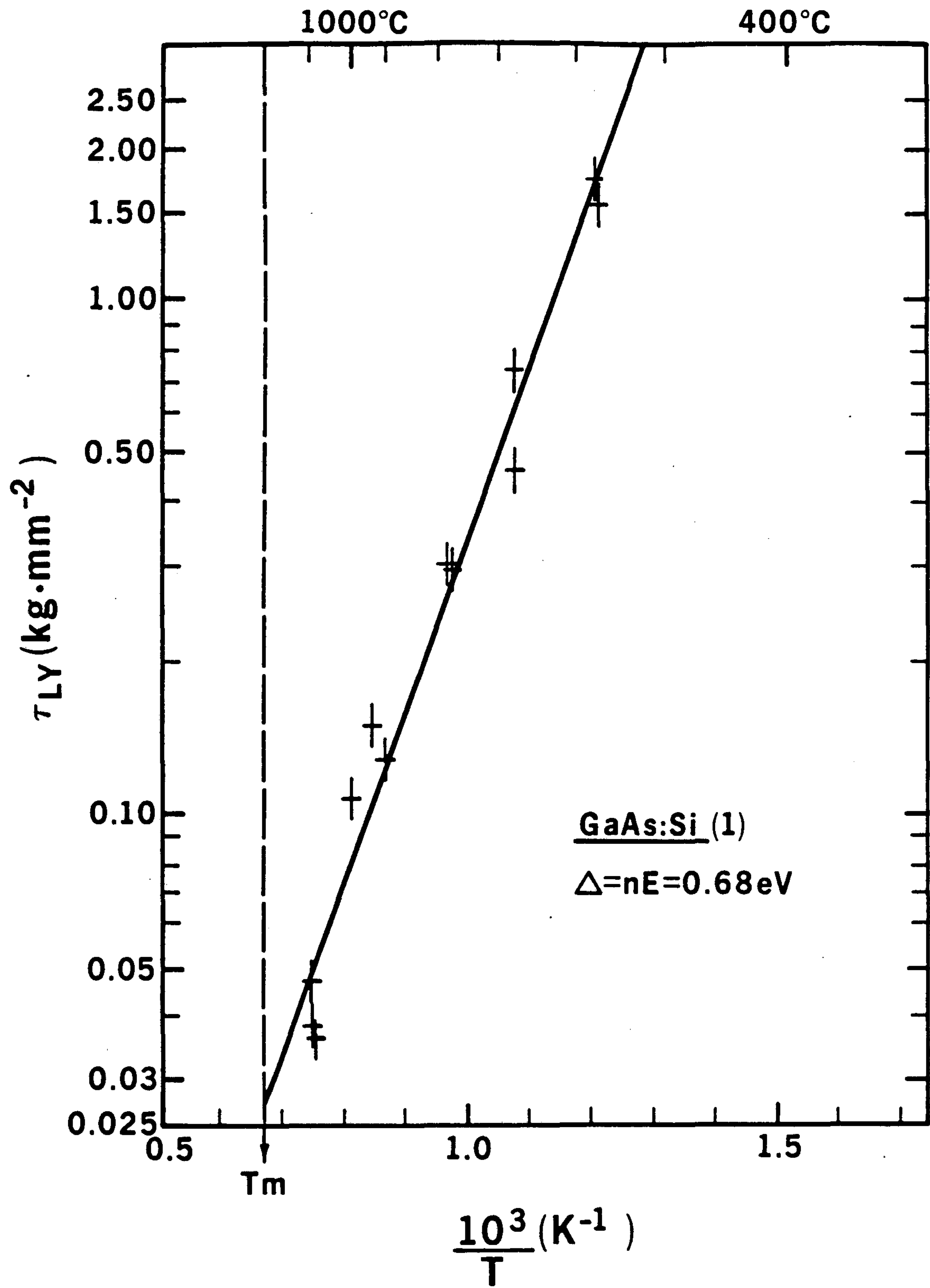

XBL 8511-4638

Fig. 18. Log(τ_{1y}) = f(1/T).
GaAs:Si (1).

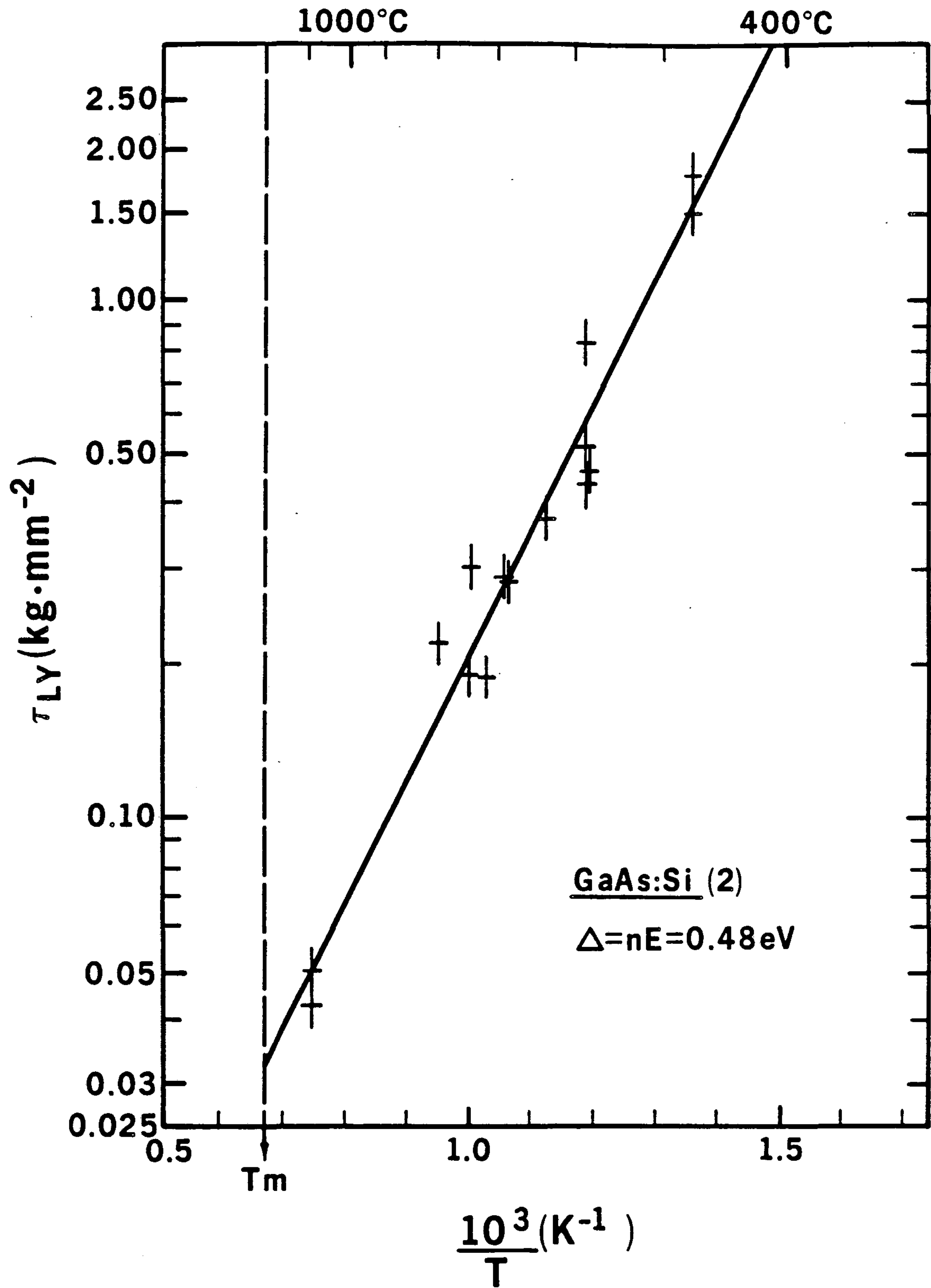

XBL 8511-4639

Fig. 19. $\text{Log}(\tau_{ly}) = f(1/T)$.
GaAs:Si(2).

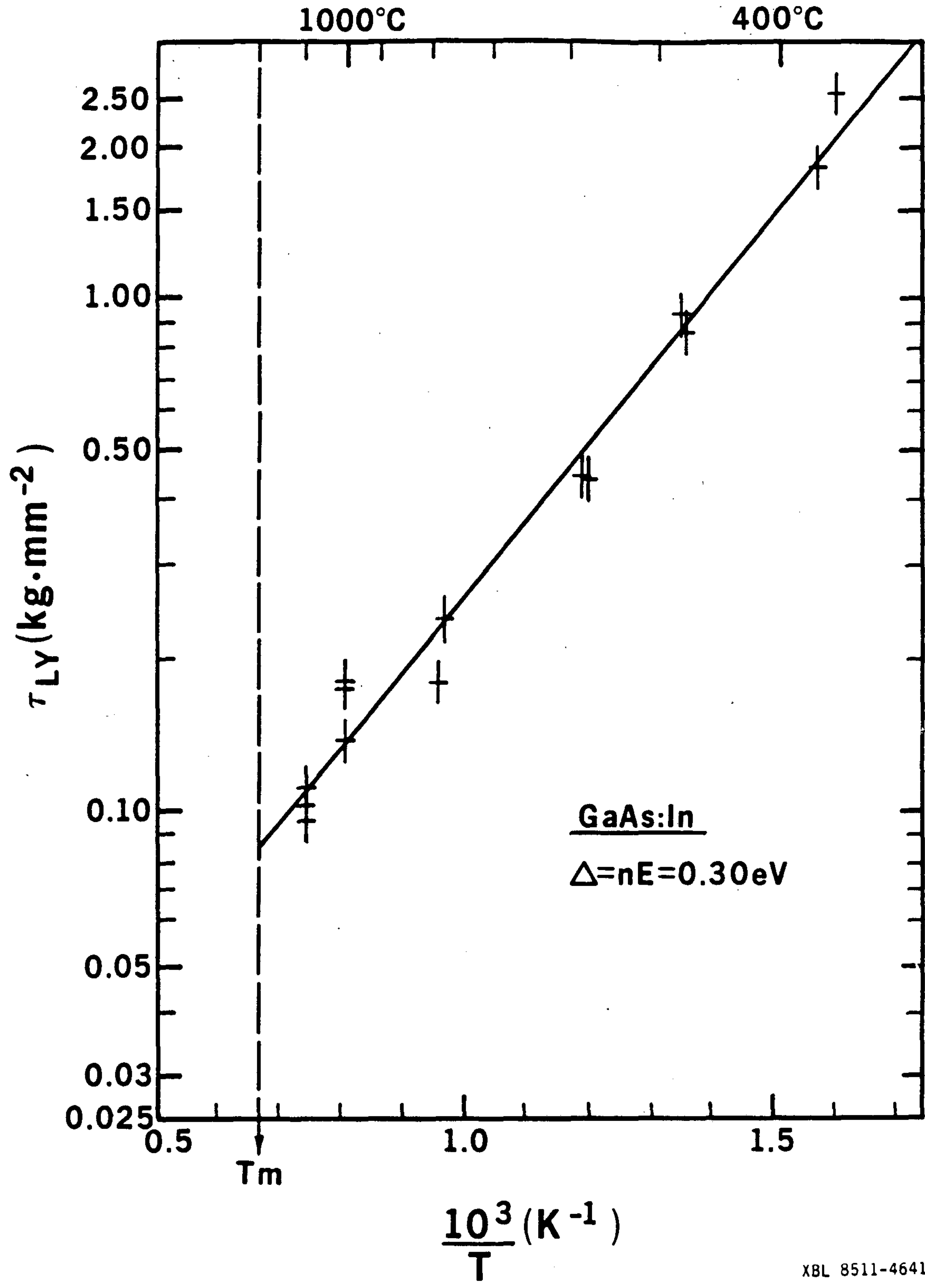

XBL 8511-4641

Fig. 20. Log(τ_{iy}) = f(1/T).
GaAs:In.

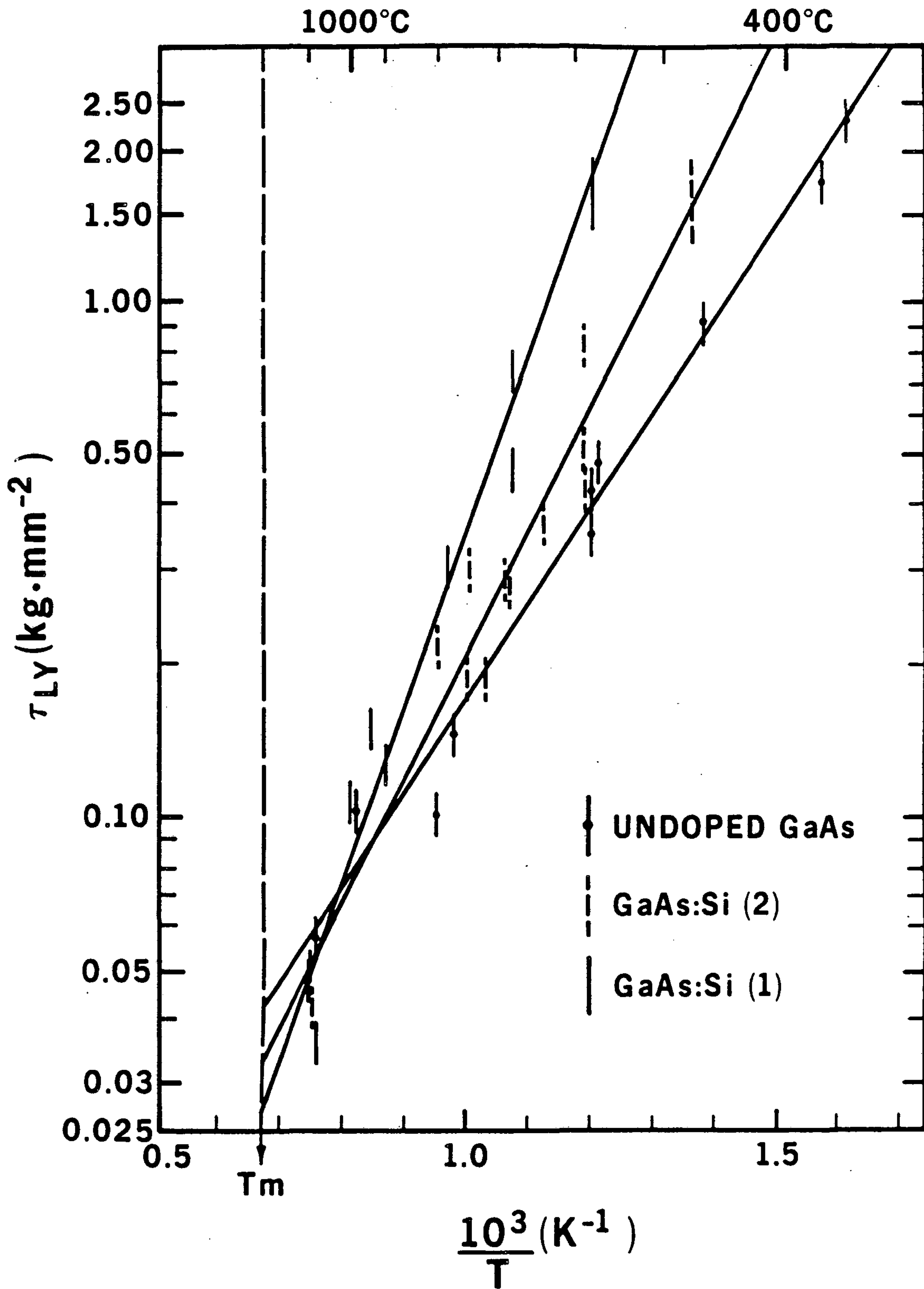

XBL 8511-4634

Fig. 21. Comparison of $Log(\tau_{ly}) = f(1/T)$ for undoped GaAs and GaAs:Si.

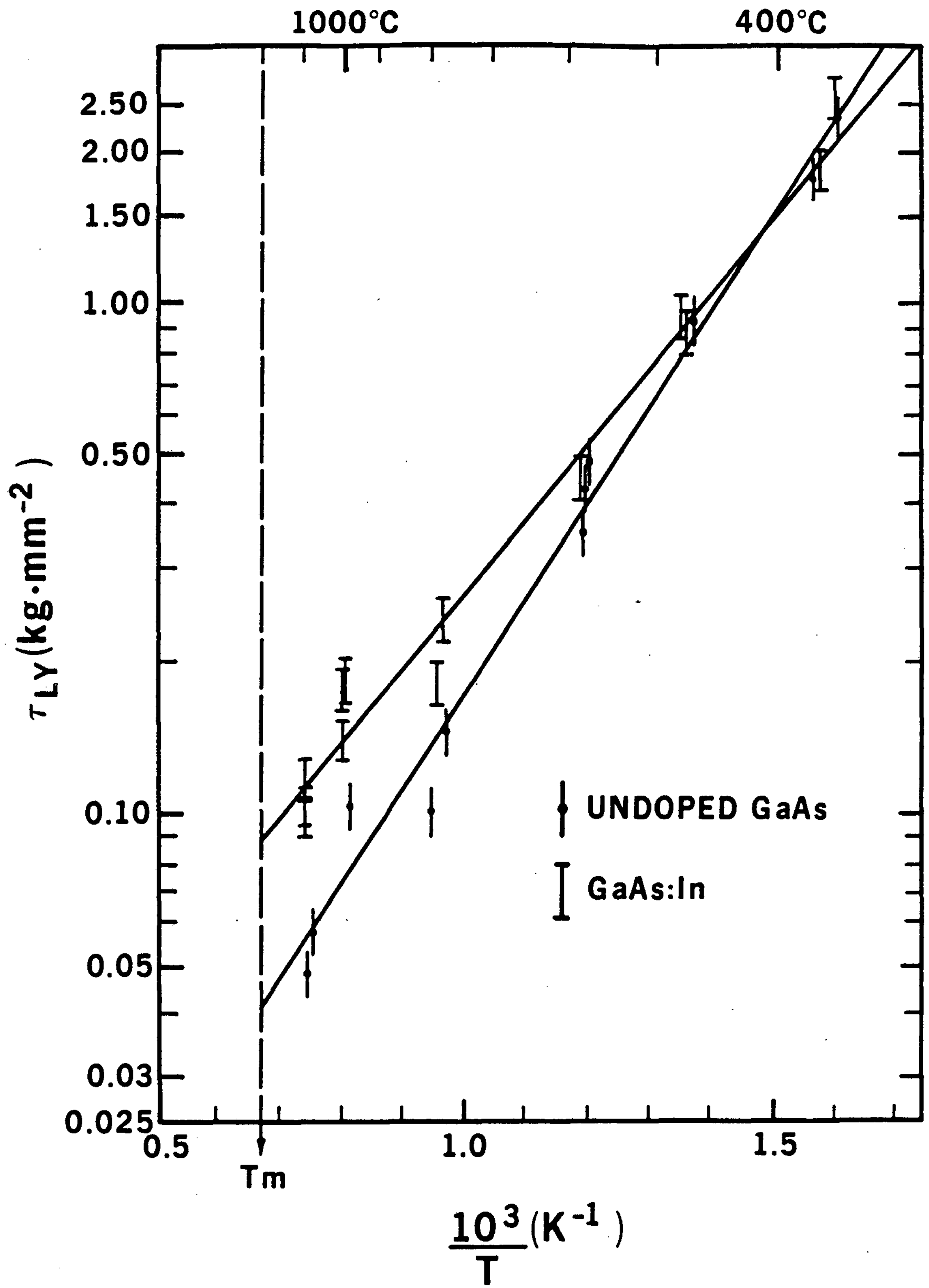

XBL 8511-4633

Fig. 22. Comparison of $\text{Log}(\tau_{ly}) = f(1/T)$ for undoped GaAs and GaAs:In.

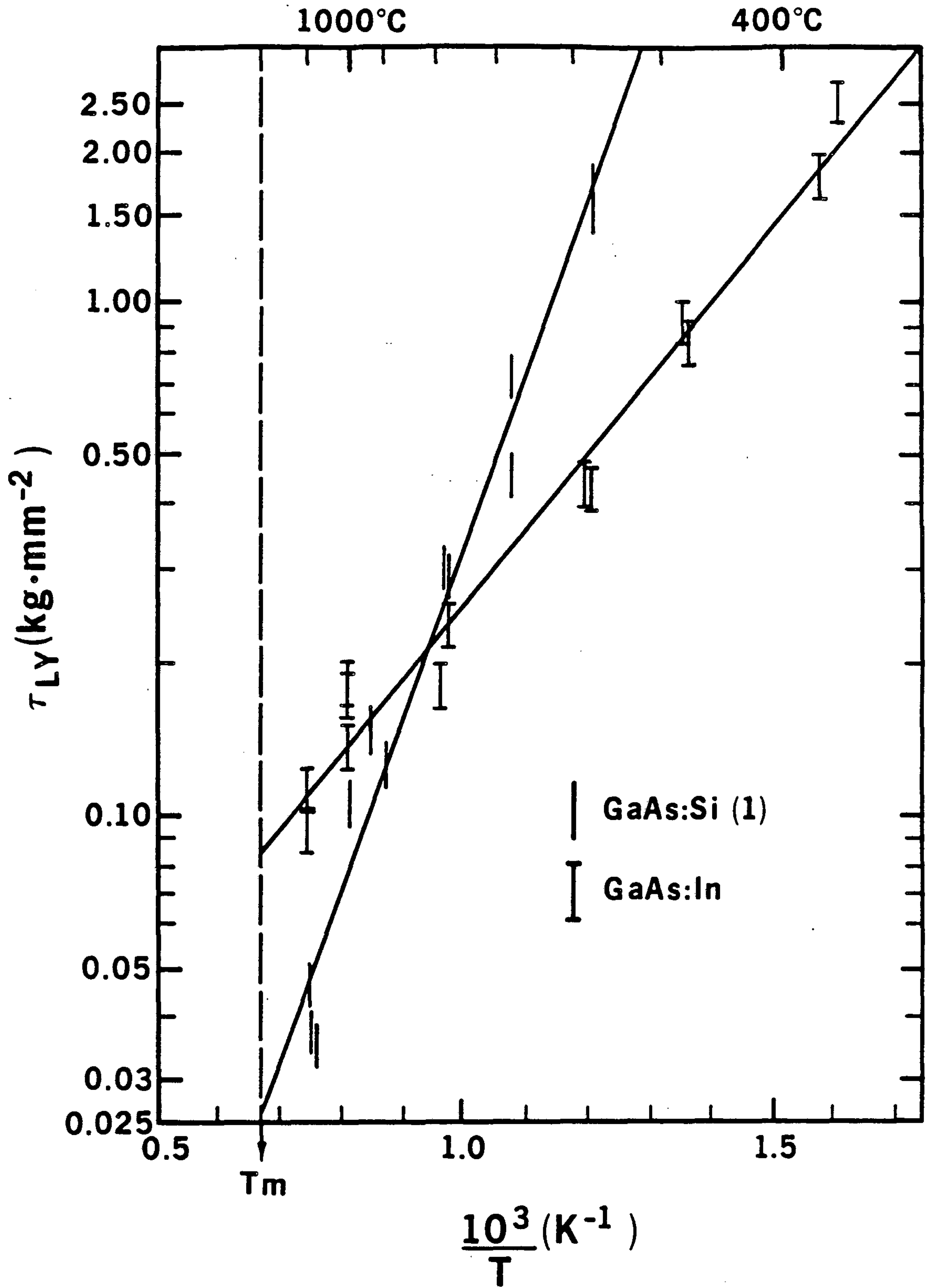

XBL 8511-4640

Fig. 23. Comparison of Log(τ_{ly}) = f(1/T) for GaAs:Si(1) and GaAs:In.

does not really matter anymore. τ_{1y} appears to describe an intrinsic characteristic of the material.

(ii) undoped GaAs and GaAs:Si: in figure 21, Log(τ_{1y}) = f(T^{-1}) is plotted for undoped GaAs, GaAs:Si(1) and GaAs:Si(2). The effect of Si doping on the deformation behavior of GaAs single crystals is very strongly temperature and concentration dependent. For both GaAs:Si, the slopes of the lines are larger than for undoped GaAs. The line corresponding to GaAs:Si(1) intercepts the line of undoped GaAs for T ≈ 1100°C. For T<1100°C, GaAs:Si(1) is harder than undoped GaAs. The temperature corresponding to this transition is T ≈ 920°C for GaAs:Si(2).

(iii) undoped GaAs and GaAs:In: the effect of In doping on τ_{1y} can be seen in figure 22. For T>390°C, GaAs:In is harder than undoped GaAs. At the melting point, the lower yield stress of GaAs:In is twice as large as that of undoped GaAs. The slope of GaAs:In is smaller, as can be best seen in the high temperature range.

Figure 23 illustrates the difference in the effect of Si and In doping on the deformation behavior of GaAs single crystals.

5. DISCUSSION

The slope of Log (τ_{1y})= f(1/T) gives an approximate value of the activation energy for the motion of dislocations (see 4.1). It appears interesting to compare the values of this activation energy E as derived from yield experiments and by velocity measurements of individual dislocations; however, as mentioned in chapter 1, three types of dislocations exist in GaAs and each type has a different velocity. A description of these dislocations follows.

5.1 Dislocations in GaAs [27]

GaAs has a zinc blende structure. The glide planes in this case are {111} and the perfect dislocations have Burgers vectors 1/2 <110>. Because of the high Peierls barrier with deep troughs along <110> directions, glide dislocations lie primarily along these directions when the dislocation density is low. Therefore, glide dislocations are either screw (i.e. $\vec{b}$ is parallel to the dislocation line) or 60° dislocations (i.e. $\vec{b}$ is inclined at an angle of 60° to the line).

Because of the double layer atomic arrangement of the diamond lattice (fig.24), there are two inherently different sets of dislocations: the glide dislocation could lie either on the narrowly spaced {111} planes (e.g. Ba plane in fig.24) or on the widely spaced {111} planes (e.g. bB in fig.24). The first set is known as the glide set and a 60° dislocation of this set can be created by removing the material bounded by the surface 1-5-6-4 and then displacing the sides of the cut so that they join. A 60° dislocation of the other set, the shuffle set, is formed in the same way but that the material cut out is bounded by the surface 1-2-3-4 (see fig.24). In both cases, the cut bonds are re-formed after the displacement, except for one bond per atom site along the dislocation line (figures 25 and 26 represent 60° dislocations in the glide set and in the shuffle set). Dislocations can transfer from one set to the other by vacancy or interstitial climb.

For GaAs, since there are two kinds of atoms in the lattice, a distinction must be made between α and β dislocations: for the α dislocation in the shuffle set, the extra-half plane of atoms ends with a Ga row and the dislocation core resembles a linear arrangement of vacancies in the As sublattice. For the β dislocation, the extra-half plane ends with a As row of atoms, and the core of the dislocation may be compared with a row of Ga vacancies [17]. α and β dislocations have opposite Burgers vectors and

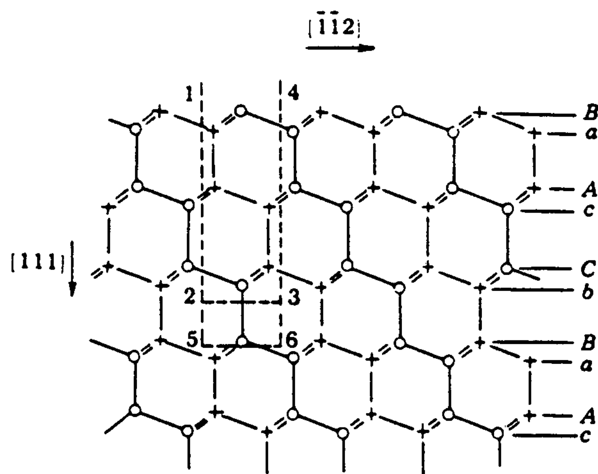

Fig. 24. A diamond cubic lattice projected normal to <$1\bar{1}0$>.
o: atoms in the plane of the paper
x: atoms in the plane below

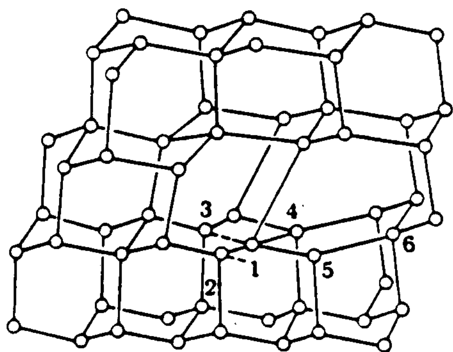

Fig. 25. 60° dislocation Glide set [27].

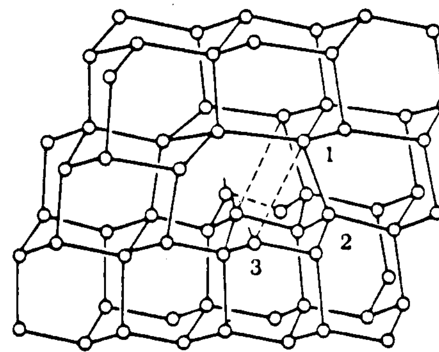

Fig. 26. 60°dislocation Shuffle set [27].

because of their different core configuration, they have different velocities. The dislocation types can be distinguished by using double-etch techniques, which take into account geometrical factors of expanding loops of dislocations. The assignements have been confirmed by x-ray topography [41].

The 60° dislocations are generally dissociated into a 30° and a 90° partials. Core reconstruction (i.e. dangling bond reconstruction) is possible with the partials, along the core for 30° partials and across the core for the 90° partials. P.B. Hirsch [20] postulates the existence of an energy band associated with the perfect dislocation; this energy level has not yet been found experimentally. According to Hirsch, the effect of reconstruction on the electronic energy levels is that the bands associated with the perfect dislocation are split into an acceptor and a donor level. At the core of the dislocation,the electron energy levels will be shifted relative to those in the perfect crystal, by amounts depending on the degree of reconstruction of the bonds. For dangling bonds in a covalently bonded solid, the energy levels are expected to be near the middle of the band gap, i.e. about midway between bonding and antibonding states. When reconstruction of the dangling bonds occurs, the electron energy levels would be expected nearer to the edges of the band gap. The position of these levels depend on the distorsion of the bonds.

The kinks that are present on the dislocation line disturb the periodicity and leads to localized electronic states in the band gap. The kinks can be reconstructed or associated with a dangling bond and thus, they introduce four electronic energy levels in the band gap (two acceptor levels and two donors) [42].

In this model, the concentration of charged kinks depends on the position of the Fermi level in the band gap.

5.2 Effect of doping on dislocation velocity

As explained in chapter 2, the velocity of dislocations in semiconductors is assumed to be proportional to the concentration of double kinks. The kinks may be neutral or charged depending on the position of the Fermi level. The total dislocation velocity is due to both charged and uncharged kinks.

Consider for example the reaction between a neutral kink K and an electron e^-:

$$K + e^- \rightarrow K^-$$

It is driven to the right by increasing the donor concentration. Since the concentration of neutral kinks is expected to be constant (at a given temperature), the total concentration of kinks increases, and so does the velocity. This model provides a mechanism for the effect of doping on dislocation velocity [20] because it describes the increase of the dislocation velocity with some dopants and the decrease of v with other dopants, depending on the accompanying changes in E_F.

Note that according to this model, only the electrical activity of the dopants matters; therefore, any donor with a "similar" electrical behavior in GaAs should have the same effect on the dislocation velocities, and isoelectronic dopants are not expected to modify these velocities.

5.3 GaAs:Si

Doping with Si obviously has an effect on the deformation behavior of GaAs single crystals: the slope of $\text{Log}(\tau_{ly}) = f(T^{-1})$ increases drastically with increasing Si concentration (see fig.21). As exposed in 4-1, this slope leads to E/(m+2), where E is the activation energy for the motion of dislocations and m is a kinetic factor characterizing the dependence of the dislocation velocity with stress. E/(m+2) = 0.37 eV for undoped GaAs and 0.48 eV for GaAs:Si(1) where [Si] = $3 \times 10^{18} cm^{-3}$.

The activation energy for dislocation motion has been determined for undoped GaAs in many studies of the deformation behavior of GaAs single crystals [10,11,13,17] and of dislocation velocities in GaAs [15,16,17]. The results of these studies are summarized in table 5. Each study was carried out under different experimental conditions and the materials differed by their growth-technique, their carrier concentrations...

From table 5, it appears that macroscopic deformations yield E values comparable to the values derived from the velocity of individual dislocations. The values of m are controversial and should be determined for each material in every experiment; for example, m increases with increasing donor concentrations [16]. We have not determined the values of m in our study, but we can evaluate a range for E for undoped GaAs:

if $m = 1$, $E = (m+2) \times 0.37 = 1.11$ eV

if $m = 2$, $E = (m+2) \times 0.37 = 1.48$ eV

These values are in quite good agreement with the results of most previous studies mentioned in table 5.

Dislocation velocity in GaAs:Si have not been measured in any of the articles given in the references. GaAs:Te is always used for the n-type material. Te is a group VI element that sits on the atom sites of the As sublattice. Si on the other hand can go on both lattices. Although these two elements occupy different sites, they both yield n-type GaAs and both Te and Si harden GaAs in the sense that they increase the values of the yield stresses. According to Hirsch's theory on the effect of doping on dislocation velocity (see 5-2), only the electrical activity of the dopants matters, since it is an electronic mechanism that controls this effect. Therefore, it is not unreasonable to compare the effects of Te and Si on dislocation velocities. Te was found to increase the

TABLE 5a.

Activation Energy for Dislocation Motion (undoped GaAs)

Deformation Tests

Material	E_{un} (eV)	m	Remarks	Ref.
undoped $n=6\text{x}10^{16}cm^{-3}$ directional crystallization initial $d_{\perp}=10^{4}cm^{-2}$	1.64±0.06	0.44	Dynamic compression tests <111> orientation T=350-650°C	[10]
undoped $n=1.5\text{x}10^{16}$-$5\text{x}10^{16}cm^{-3}$ gradient freeze	2.56±0.05	0.37	4-point bending T<700°C (static) Dynamical tension tests for T>700°C	[11]
undoped $n=35\text{x}10^{16}cm^{-3}$ directional crystal initial $d_{\perp}=10^{4}cm^{-2}$	1.45	1.2	bending (3-point bending) (static) T=400°C-650°C <110> bending axis =2-9 kg/mm^{-2}	[13]
undoped $n=10^{17}cm^{-3}$	1.5		uniaxial compression (static) at =1 kg/mm^{-2}, <123> orientation T=300-700°C	[17]

TABLE 5b.

Activation Energy for Dislocation Motion (undoped GaAs)
Dislocation Velocity Measurements

Material	E_{un} (eV)	m	Remarks	Ref.
undoped n=1.3x10^{16}cm^{-3}	E_{α}-0.93		4-point bending and double etching	
initial $d_{\perp}$=10^{13}cm^{-2}	E_{β}-1.57		<111> stretched face	[15]
	E_S=1.11		T=200-450°C	
			=2 kg/mm^{-2}	
undoped n=10^{17}cm^{-3}	E_{α}=1.0	1.4	3-point bending and double-etching	
initial $d_{\perp}$=10^{3}cm^{-2}	E_{β}=1.35	1.6	=2 kg/mm^{-2}	[16]
undoped n=10^{17}cm^{-3}	E_{α}=1.2		uniaxial compression and double etching	
			<123> orientation	
			=2 kg/mm^{-2}	[17]

TABLE 6a.

Activation Energy for Dislocation Motion (GaAs:Te)
Deformation Tests

Material	E_n (eV)	m	Ref.
GaAs:Te $n=8.8\times10^{18}cm^{-3}$	2.66±0.06	2.17	[10]
GaAs:Te $n=2.3\times10^{17}-17\times10^{18}cm^{-3}$	4.15±0.05	3.7	[11]
GaAs:Te $n=1.9\times10^{18}cm^{-3}$	2.30	1.5	[13]
GaAs:Te $n=2.3\times10^{18}cm^{-3}$	2.2		[17]

TABLE 6b.

Activation Energy for Dislocation Motion (GaAs:Te)
Dislocation Velocity Measurements

Material	E_n (eV)	m	Ref.
GaAs:Te	$E_\alpha=1.03$		
$n=8\times10^{18}cm^{-3}$	$E_\beta=1.42$	2.1	
	$E_s=1.25$		[15]
$n=3.5\times10^{19}cm^{-3}$	$E_s=1.25$	2.4	
GaAs:Te $n=2.3\times10^{18}cm^{-3}$	$E=1.8$		[17]

activation energy for dislocation motion as compared with undoped GaAs, as can be seen in table 6.

The values of m have been found to increase with increasing dopant concentration [15,16]. Even if the value of m has not been determined for GaAs:Si in our experiments, one may suppose that m is larger for the Si-doped material than for the undoped material. Since E/(m+2) is larger for GaAs:Si (0.68 eV for GaAs:Si(1) and 0.48 eV for GaAs:Si(2) to be compared with 0.37 eV for undoped GaAs), we may conclude that E is increased with Si doping. Therefore, the dislocations in GaAs:Si have a smaller velocity than in undoped GaAs and the arrangement of the dislocations on the {111} etched slices confirm this hypothesis: the dislocations are not aligned on slip lines at the periphery of the GaAs:Si slice as they are for the undoped GaAs. In conclusion, it may be said that the dislocations freshly introduced during the compression tests do not propagate as easily in GaAs:Si as they do in undoped GaAs.

As can be seen in figure 21, the addition of Si in GaAs also increases the value of the lower yield stress compared to the undoped GaAs. If we define hardening as an increase of the lower yield stress, then GaAs:Si (1) is harder than undoped GaAs for $T<1110^{\circ}C$ and GaAs:Si (2) is harder for $T<920^{\circ}C$. These temperatures probably correspond to the temperatures where the intrinsic carrier concentration become comparable to the concentrations of electrically active Si.

Swaminathan and Copley [12] are the only authors who studied the deformation behavior of Si-doped GaAs; their material was grown by the Bridgman technique and $[Si] = 1.8 \times 10^{18} cm^{-3}$. They performed repeated-yielding experiments in compression, at a constant-force rate; they report that the addition of Si increases the yield stress with respect to the undoped material. Although their experimental approach is

very different from ours, we may compare the numerical values of their yield stress σ with our lower yield stress for GaAs:Si(2) which has a comparable Si concentration:

T = 400°C

$\sigma_{un} = 3.83(kg/mm^{-2})$ $\qquad \tau_{ly} = 1.42(kg/mm^{-2})$

$\sigma_{Si} = 5.32(kg/mm^{-2})$ $\qquad \tau_{ly} = 3.32(kg/mm^{-2})$

T = 550°C

$\sigma_{un} = 1.49(kg/mm^{-2})$ $\qquad \tau_{ly} = 0.42(kg/mm^{-2})$

$\sigma_{Si} = 1.91(kg/mm^{-2})$ $\qquad \tau_{ly} = 0.72(kg/mm^{-2})$

The values derived in [12] are higher than ours, partly because the strain-rate corresponding to their experiments is higher than ours : $8.3 \times 10^{-4}s^{-1}$ in [12] compared to $10^{-4}s^{-1}$ in our experiments.
Also, the yield stress values obtained by repeated-yielding are increased to some degree by strain-hardening. In any case, the stress values are of the same order and a hardening effect of Si is observed in this range of temperatures.

At temperatures close to the melting point, GaAs:Si is softer than undoped GaAs (fig.21). If the CRSS introduced in 2.1 is taken equal to the lower yield stress, then the formation of dislocations by crystallographic glide during the LEC growth of GaAs, should be easier in GaAs:Si(1) and GaAs:Si(2) as compared to undoped GaAs:

at T_m $\quad \tau_{ly}$ (undoped GaAs) = $40.77\ g/mm^{-2}$

τ_{ly} (GaAs:Si (1)) = $26.95\ g/mm^{-2}$

τ_{ly} (GaAs:Si (2)) = $32.43\ g/mm^{-2}$

However, GaAs:Si(1) is dislocation-free, whereas GaAs:Si(2) has a dislocation density comparable to that of the undoped GaAs. Two hypotheses can be made here: a) the dislocations are formed at lower

temperatures than the melting point during the growth process. In the temperature range 920°C-1100°C, GaAs:Si(1) is harder than undoped GaAs, whereas GaAs:Si(2) is softer than undoped GaAs. This could explain why GaAs:Si(2) has the same dislocation density as undoped GaAs. b) the formation of dislocations during the growth of Si-doped GaAs is not governed by the thermal stresses, but rather by the native defects, which are strongly affected by the silicon doping. In the case of GaAs:Si(2), although the concentration of Si is large enough to affect the motion of the dislocations introduced in the deformation process, it may not affect the mobility and precipitation of native defects and thus, the generation of dislocations during growth. The electronic effect of Si doping on the motion of freshly introduced dislocation is dominant in the deformation process and could hide other effects that are prevalent during the actual growth.

5.4 GaAs:In

As mentioned earlier, there are no reports of deformation studies of GaAs:In. In figure 22, Log(τ_{1y}) is plotted as a function of T^{-1} for both the undoped GaAs and GaAs:In. It can be seen from this graph that the addition of In increases τ_{1y} for T>390°C, and decreases the slope of Log (τ_{1y}) = f(T):

E/(m+2) = 0.30 ± 0.01 eV for GaAs:In and E/(m+2) = 0.37 ± 0.02 eV for undoped GaAs. The value of m for GaAs:In has not been reported anywhere. At this point, we are unable to say if this difference is due to a different E or a different m. A recent study finds that In does not show any effect on the dislocation velocity [43]. The LEC grown GaAs:In tested in [43] had a dopant concentration of 8.2-12 x 10^{19} cm^{-3} and the material was initially dislocation-free. The specimens were placed

under stress (3-point bending) after a scratch was made on the (111) As surface of the samples. The velocity of the dislocation was determined by the double-etch technique and displacements of dislocations caused by shear stresses between 0.4 to 4 kg/mm^{-2}, at temperatures between 190°C and 450°C were measured for α and β dislocations. The activation energy for the motion of dislocations was calculated for velocity measurements at $\tau = 2$ kg/mm^{-2} and T=190-450°C. Note that the authors report a 30 % scatter of the velocities. The results of this study are:

$E_\alpha = 0.89$ eV and $E_\beta = 1.24$ eV for both the undoped and the In doped samples. Figure 27 is a plot of Log(v) as a function of the resolved shear stress as reproduced from [43]. The value of m is given by the slope of these lines and our estimation of this slope is m = 2.1, at T = 300°C. From E/(m+2) = 0.30 eV and m = 2.1, we can estimate E for GaAs:In :

$$E = 4.1 \times 0.30 = 1.23 \text{ eV}$$

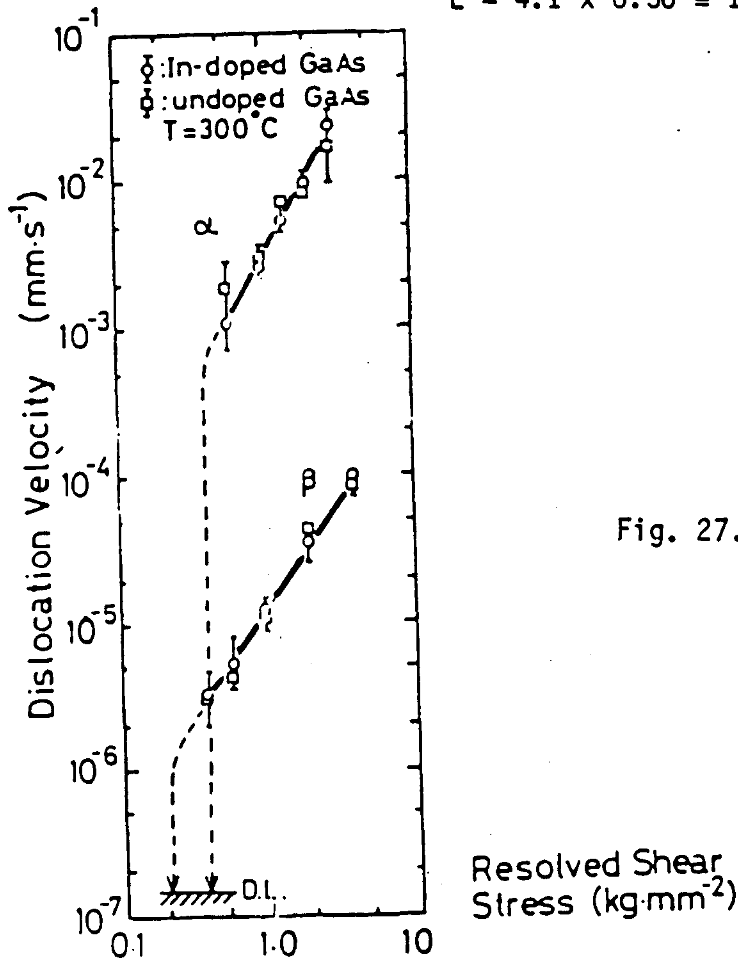

Fig. 27. Log(v) = f(τ) [44]
The slope of the lines is equal to m.

It must be noted here that no substantial change in the activation energy for dislocation motion was observed with high concentrations ($\approx 5 \times 10^{20}$ cm^{-3}) of isoelectronic doping in Silicon [31]. Another interesting observation is that the model of the effect of doping on dislocation velocities exposed in 5-2, predicts no effect of isoelectronic doping.

Therefore, it seems reasonable to assume that the results of Matsui et al, [43] are correct. It means that the addition of In has a very little effect on the motion of freshly introduced dislocations, in the 190°C-450°C temperature range; thus, there is no or little interaction between the solute atoms and the newly introduced dislocations at these temperatures, and indeed, it is possible that no effect of In-doping on the deformation behavior of GaAs will be observed. Unfortunately, our tests cannot be successfully carried out at lower temperatures because the samples break before the yield points are reached. . Our data shows however a hardening effect for T>400°C, and we cannot exclude the possibility that In does affect the dislocation motion for these higher temperatures; further studies are needed to clarify this point.The fact remains that Indium reduces the grown-in dislocation densities very efficiently.

Ehrenreich and Hirth [44] analyzed this effect on the basis of a solid solution hardening model. If GaAs:In is described in terms of $InAs_4$ tetrahedral "solute" defects in a GaAs matrix, the addition of In creates a size misfit of 21 % . The elastic interaction energy between a misfitting volume and an edge dislocation is calculated in this model. From this interaction energy, the resolved shear stress needed to break

the dislocation away from the solute pinning points can be derived. At room temperature, the break-away stress for a 3 % In concentration material is found to be roughly four times the yield stress of undoped GaAs as determined by Swaminathan and Copley [12]. This result is inconsistent with the fact that dislocation velocities are equal in GaAs:In and undoped GaAs for T<450°C, because solution hardening involves pinning of the dislocations at solute points and therefore, the velocities should be reduced by the addition of In.

Solution hardening is also found incompatible with conclusions from a study of melting processes in undoped and In-doped GaAs. Sato et al, [45] observed melting processes of these two materials by live x-ray topography with synchrotron radiation. They noted that melting starts preferentially in regions where there is a surface accumulation of In, because of local lowering of the melting point. However, the melting does not start preferentially from heavily dislocated areas, which indicates that In concentration around the dislocations is nearly the same as in the dislocation-free areas. Therefore, the interactions of dislocations with In atoms are thought to be very weak near the melting point. The authors conclude that "simple" solution hardening [45] or dragging of dislocations by In atmosphere [6] should not be expected at high temperatures. In summary, we can say that the addition of Indium hardens the GaAs lattice for T>400°C, but it is not quite clear if the hardening mechanism is actually solution hardening.

Sato, et al. also report that marked differences in the generation of dislocation by slip are observed between the HB grown undoped GaAs and the LEC grown GaAs:In. During heating, slip bands are generated in the <110> direction by thermal stresses; in undoped GaAs, for T>1000°C,

dislocations are created and they multiply from both sides of the slip band. Such processes are not clearly observed in the GaAs:In specimens.

In view of all this information, and considering the fact that Indium does reduce dislocation densities in LEC GaAs, we may suppose that the addition of In affects the generation processes of dislocations during LEC growth as well as the propagation processes. The generation processes, presented in chapter 2, are: crystallographic glide caused by thermal stresses, condensation of native defects and non-stoichiometry. Alloying with In certainly modifies all three processes, since they are intimately related. From figure 22, it can be seen that GaAs:In has a higher τ_{ly} for high temperatures (T>400°C) than undoped GaAs. If τ_{ly} at T_m is a good approximation for CRSS, then the admissible levels of thermal stresses during the growth can be higher when In is added to the melt and crystallographic glide is less likely than in undoped GaAs:

$$\text{at } T_m, \quad \tau_{ly} \text{ (undoped GaAs)} = 40.77 \text{ g/mm}^{-2}$$

$$\tau_{ly} \text{ (GaAs:In)} = 81.86 \text{ g/mm}^{-2}$$

It is only a two-fold increase of the CRSS, and it is unlikely that the reduction of grown-in dislocation densities is due to this sole effect.

Indium could also affect the generation of dislocations by modifying the nature and concentration of native defects. In a recent article, Sher, et al. [46] claim that the rate of dislocation formation by vacancy condensation is slower in an alloy where the added constituent has a shorter bond length. In such an alloy, the average bond length is smaller than in the unalloyed material; according to the authors, this does not affect the equilibrium vacancy density but rather the rate at which vacancies anneal or condense into dislocations, due to a higher energy of formation of these dislocations. The dislocation energy per

unit length is found to be proportional to d^{-3}-d^{-9}, where d is the average bond length.

So, alloying a semiconductor with another element with a shorter bond length is a strategy for reducing grown-in dislocation densities. This result suggests that adding a small amount of GaP to GaAs may significantly reduce the dislocation density: in GaP, d = 2.359 Å , whereas in bulk grown GaAs, d = 2.448 Å . However, Jacob who grew P-doped GaAs [5] reports that the grown-in dislocation densities were comparable to the undoped case (see table 1). There is another incoherence in this model: the addition of In has the effect of increasing the average bond length (d_{InGa} = 2.623 Å). The authors explain that the longer InAs bond causes GaAs bonds in the neighborhood to be compressed and they expect this mechanism to be less effective than substituting short bond-length additives. However, In is probably one of the most efficient dopant in regard to reducing grown-in dislocation densities.

Even if this model is not entirely satisfying, it brings up a new idea: the reduction of dislocation densities could be based on the effects of doping on the generation processes, rather than on changes in the dislocation velocities. The addition of a dopant certainly modifies the concentrations and mobilities of native defects. The latter play an important role in the generation of dislocations during growth: not only do they move and possibly condensate into dislocations, but they also affect the stoichiometry of the crystals. In particular, Ga vacancies stand out as a very relevent defect [26]. Indium being a group III element, will sit on the Ga sites and probably change the concentration and/or the mobility of the Ga vacancies.

The minimum Si concentration needed to see an appreciable decrease in the grown-in dislocation densities is $\simeq 3 \times 10^{18}$ cm^{-3}, whereas the corresponding In concentration is $\simeq 2 \times 10^{19}$ cm^{-3}, which means that roughly 10 times more In is required to have the same effect as Si. As mentioned in 5-3, Si atoms can occupy both Ga and As sites but the ratio Si_{As}/Si_{Ga} is of the order of 0.2-0.4 [47]. So, it seems reasonable to conclude that the mechanisms of dislocation density reduction are different when GaAs is doped with Silicon or with Indium. In fact, to compare the effects of different dopants on the deformation behavior of GaAs single crystals, the segregation coefficient and the distribution of the atoms on the two sublattices should be considered. Crystals with an equal concentration of dopants on the Ga sublattice could then be tested. One difficulty remains: Si is electrically active whereas In is not; the effect of Si doping on dislocation velocities will always be superimposed and apparently, it is the dominant effect. It would be interesting at this point to test GaAs doped with Si and another acceptor impurity --such as Zn for example--that would compensate the electrical activity of Si.

6. SUMMARY AND CONCLUSIONS

Undoped, Silicon and Indium doped GaAs single crystals have been tested in dynamical compression tests at constant strain-rate. The temperatures ranged from 350°C to 1100°C. For T>800°C, the samples were encapsulated in B_2O_3. All the crystals used in this study were LEC grown, and their thermal history was identical, to minimize the differences in the initial defect content. The natural logarithms of the lower yield

stresses are plotted as a function of T^{-1}. The conclusions can be summarized as follows:

(1) <u>GaAs:Si</u>

- The deformation behavior of Si doped GaAs is strongly dependent on the Si content.

- GaAs:Si is harder than undoped GaAs for low temperatures and softer near the melting point.

- Si doping decreases the velocity of the dislocations introduced during plastic deformation as compared to the undoped case. The mechanism of this effect can be understood on the basis of the electrical activity of Silicon in GaAs. The presence of Si atoms changes the concentration and mobility of kinks on the dislocation lines. The decrease of the dislocation velocities could explain the reduction of grown-in dislocation densities in LEC GaAs:Si. This explanation is not entirely satisfying however, and we have to consider the possibility that Si reduces the dislocation densities by another mechanism, via native defects spectrum, concentration and mobility.

(2) <u>GaAs:In</u>

- Indium doping hardens the GaAs lattice for T>400°C, but its effects at T<400°C are not clearly observed. The results of a recent study of dislocation velocities in GaAs:In seem to indicate that In does not modify the motion of dislocations for T<450°C.

- Although a study of the melting processes of undoped and In-doped GaAs suggests that there are no interactions between In atoms and dislocations near the melting point, solution hardening cannot be ruled out to explain the hardening effect of In for T>400°C.

- We speculate that the reduction of grown-in dislocation densities by addition of In is due to an effect of In on the generation processes during LEC growth, as opposed to propagation processes.

- GaAs:In is twice as hard as undoped GaAs at the melting point. This result means that the CRSS for crystallographic glide is larger in GaAs:In than in undoped GaAs.

- We suggest however that the reduction of grown-in dislocation densities by addition of In in the melt is due to an effect of In on the native defects. This effect is probably different from the effect of Si doping, since ≈ 100 times less Si than In is required to markedly affect the dislocation densities.

REFERENCES

1. J.V. DiLorenzo, A.S. Jordan, A.R. Von Neida and P. O'Connor in "Semi-Insulating III-V Materials", Kah-nee-ta 1984, p. 308, eds. D.C. Look and J.S. Blakemore, Shiva Pub. U.K.

2. S. Miyazawa, Y. Ishida and Y. Nanishi, Appl. Phys. Lett., 43 (1983) 11

3. R.K. Willardson in "Semi-Insulating III-V Materials", Kah-nee-ta 1984, p. 97, eds. D.C. Look and J.S. Blakemore, Shiva Pub., U.K.

4. J.M. Parsey, Y. Nanishi, J. Lagowski and H.C. Gatos, J. Electrochem. Soc. 128 (1981) 1346.

5. G. Jacob in "Semi-Insulating III-V Materials", Evian 1982, p. 2, eds. S. Makram-Ebeid and B. Tuck, Shiva Pub., U.K.

6. M.G. Mil'vidskii, V.B. Ovenskii and S.S. Shifrin, J. Cryst. Growth 52 (1981) 396.

7. M. Duseaux and S. Martin in "Semi-Insulating III-V Materials", Kah-nee-ta 1984, p. 118, eds. D.C. Look and J.S. Blakemore, Shiva Pub., U.K.

8. H.M.Hobgood in "Semi-Insulating III-V Materials", Kah-nee-ta 1984,p. 149, eds. D.C. Look and J.S. Blakemore, Shiva Pub., U.K.

9. J.R. Patel and A.R. Chadhuri, Phys.Rev., 143(2) (1966) 601.

10. N.P. Sazhin, M.G. Mil'vidskii, V.B. Ovenskii and O.G. Stolyarov, Sov. Phys. Solid State, 8(5) (1966)1223.

11. D. Laister, G.M. Jenkins, J. of Mat. Sc., 8 (1973) 1232.

12. V. Swaminathan and S.M. Copley, J. of Amer. Ceram. Soc., 58 (1975) 482.

13. V.B. Ovenskii, M.G. Mil'vidskii and O.G. Stolyarov, Sov. Phys. Solid state, 13(5) (1969) 718.

14. V.B. Ovenskii and L.P. Kholodnyi, Sov. Phys. Solid State, 14(11) (1973) 2822.

15. V.B. Ovenskii, L.P. Kholodnyi and M.G. Mil'vidskii, Sov. Phys. Solid State, 15(3) (1973) 661.

16. S.K. Choi, M. Mihara and T. Ninomyia, Jap. J. of Appl. Phys., 16(5) (1977) 737.

17. H. Steinhardt and P. Haasen, Phys. Stat. Sol. (a), 49 (1978) 93.

18. S.A. Erofeeva and Yu.A. Ossipyian, Sov. Phys. Solid State, 15(3) (1973) 538.

19. Y. Seki,H. Watanabe and J. Matsui, J. of Appl. Phys., 49(2) (1978) 822.

20. P.B. Hirsch, J. de Phys., Colloque C6, supplement au n°6, 40 (1979)117.

21. R. Jones, J. de Phys., Colloque C4, supplement au n°9, 44 (1983) 61.

22. A.S. Jordan, R. Caruso and A.R. Von Neida, The Bell System Technical Journal, 59(4) (1980) 593.

23. M. Duseaux and G. Jacob, Appl. Phys. Lett., 40(9) (1982)790.

24. M. Duseaux, J. of Crys. Growth, 61 (1983) 576.

25. J.C. Brice and G.D. King, Nature, 209 (1966) 1346.

26. J. Lagowski, H.C. Gatos and D.G. Lin in "Semi-Insulating III-V Materials", Kah-nee-ta 1984, p. 60, eds. D.C. Look and J.S. Blakemore, Shiva Pub., U.K.

27. J.P.Hirth and J. Lothe,"Theory of dislocations" second edition (1982) J. Wiley and sons.

28. R.E. Peierls, Proc. Phys. Soc., 52 (1940) 23.

29. H. Alexander and P. Haasen, Sol. State Phys., 22 (1968) 27.

30. V. Celli, M. Kabler, T. Ninomiya and R. Thomson, Phys. Rev., 131(1) (1963) 58.

31. V.N. Erofeev and V.I. Nikitenko, Sov. Phys. Solid State, 13(1) (1971) 116.

32. K. Sumino, Colloque C6, supplement au n°6, 40 (1979) 147.

33. G. Jacob, J.P. Farges, M. Duseaux, J. Hallais, W.J. Bartels and P.J. Roksnoer, J. of Cryst. Growth, 57 (1982) 245.

34. see for example C.N. Reid, in "Deformation Geometry for Materials Scientists", Int. Series on Mat. Science and Technology, vol II. Ed. W.S. Owen, Pergamon Press (1973).

35. E. Orowan, Proc. Phys. Soc. (London), 52 (1940) 8.

36. P. Haasen, Z. Physik, 167 (1962) 461.

37. W.G Johnston, J. of Appl. Phys., 33 (1962) 2716.

38. M.G. Mil'vidskii and E.P. Bochkarev, J. of Cryst. Growth, 44 (1978) 61.

39. G. Muller, R. Rupp, J. Volkl, H. Wolf and W. Blum, J. of Cryst. Growth, 71 (1985) 771.

40. P. Haasen, private communication.

41. M. Mihara and T. Ninomyia, Phys. Stat. Sol.(a), 32 (1975) 43.

42. P.B. Hirsch in "Fundamentals of Deformation and Fracture", eds.B.A. Bilby, K.J. Miller and J.R. Willis, Cambridge U. Press (1985).

43. M. Matsui and T. Yokoyama, presented at the "12th International Symposium on GaAs and related compounds", sept. 1985, Karuizawa, Japan.

44. H. Ehrenreich and J.P. Hirth, Appl. Phys. Lett., 46(7) (1985) 668.

45. F. Sato, M. MAtsui and J. Chikawa, presented at the "12th International Symposium on GaAs and related compounds", sept. 1985, Karuizawa, Japan.

46. A. Sher, A.B. Chen and W.E. Spicer, Appl. Phys. Lett., 46(1) (1985) 54.

47. J.B. Mullin, A. Royle and S. Benn, J. of Cryst. Growth, 50 (1980) 625.

This report was done with support from the Department of Energy. Any conclusions or opinions expressed in this report represent solely those of the author(s) and not necessarily those of The Regents of the University of California, the Lawrence Berkeley Laboratory or the Department of Energy.

Reference to a company or product name does not imply approval or recommendation of the product by the University of California or the U.S. Department of Energy to the exclusion of others that may be suitable.

LAWRENCE BERKELEY LABORATORY
TECHNICAL INFORMATION DEPARTMENT
UNIVERSITY OF CALIFORNIA
BERKELEY, CALIFORNIA 94720